Environmentally friendly corrosion resistant coatings as alternatives for cadmium and chromium in the aerospace industry

Masters Thesis

by

Ivan Huysamen

A thesis submitted in partial fulfillment of the requirements for the degree of

MASTER OF ENGINEERING

in

METALLURGICAL ENGINEERING

from the department of

MATERIALS SCIENCE AND METALLURGICAL ENGINEERING

of

THE UNIVERSITY OF PRETORIA

October 2017

Abstract

European REACh regulations are aimed at the complete removal of the toxic and carcinogenic cadmium and hexavalent chromium coatings currently being employed for corrosion protection of ultra-high strength steel and other aviation components. A powdered aluminium alloy containing 12 mass % manganese, applied with atmospheric plasma spraying, were tested as a possible alternative to cadmium electroplating. Complemented with the development of a permanganate-vanadate based conversion coating as an alternative to the Cr^{VI} based treatment. The plasma sprayed AlMn12 alloy had very good electrochemical properties and medium term corrosion resistance, but did not pass the bend adhesion test. The Mn-V conversion coating showed much promise, as it performed similarly/better than a commercial Cr^{III}-Zr coating in short and medium term corrosion tests. Further additional tests and process refinement are still required, but the Mn-V coating clearly has significant potential as a possible future alternative to chromate conversion coating.

Contents

List of Figures

List of Tables

List of Acronyms

APS	Atmospheric Plasma Spraying
ASNS	American Society for Nutritional Science
ASTM	American Society for Testing and Materials
ATSDR	Agency for Toxic Substances and Disease Registry
BASF	Badische Anilin und Soda Fabrik
BSAA	Boric Sulphuric Acid Anodizing
CAA	Chromic Acid Anodizing
CCC	Chromate Conversion Coating
CVD	Chemical Vapour Deposition
DoD	Department of Defence
ECHA	European Chemicals Agency
ED	Electro Deposition
EDX	Energy Dispersive X-Ray
ELV	End-of-Life Vehicle
EIC	Environmentally Induced Cracking
FCC	Face Centred Cubic
HVOF	High-Velocity OxyFuel
IARC	International Agency for Research on Cancer
ISO	International Organization for Standardization
IVD	Ion Vapour Deposition

NATO	North Atlantic Treaty Organization
NDCEE	National Defence Centre for Environmental Excellence
NEHC	Navy Environmental Health Centre
OSHA	Occupational Safety and Health Administration
PCC	Permanganate Conversion Coating
PEL	Permissible Exposure Limit
PEO	Plasma Electrolytic Oxidation
PMB	Plastic Media Blasting
PSD	Particle Size Distribution
PVD	Physical Vapour Deposition
REACh	Registration, Evaluation, Authorisation and Restriction of Chemicals
RoHS	Restriction on the use of Hazardous Substances
SCE	Standard Calomel Electrode
SHE	Safety Health and Environment
SME	Small and Medium-sized Enterprises
SVHC	Substance of Very High Concern
TSA	Tartaric Sulphuric Acid
UMS	Unbalanced Magnetron Sputtering
UTS	Ultimate Tensile Strength

1 Cadmium based corrosion protection

1.1 Introduction

Globally there is an increasing drive for all industrial processes and the resulting products to be more environmentally friendly, as resources should be utilized in such a way as to allow re-use and recycling of products at the end of their life cycles, while their production remains efficient and generates as little waste as possible.

In Europe new programmes and legislation such as REACh (Registration, Evaluation, Authorisation and Restriction of Chemicals)[1], ELV (End-of-Life Vehicle)[2] and RoHS (Restriction on the use of Hazardous Substances)[2,3] are the main driving forces behind the decreased reliance and future elimination of toxic/hazardous heavy metals from industry. This not only impacts European nations, but also other countries around the world with which manufacturing partnerships are shared. The aviation industry is a prime example of such a partnership due to the large number of components and materials utilized in the construction of aircraft, which regardless of the applicable local environmental rules of the country of origin, requires components to be manufactured to European specifications. As a result corrosion protection of steel airplane components using cadmium coatings, electrodeposited from cyanide solutions and passivated with a hexavalent chromium post-treatment, is one of the long standing processes that has come under intense pressure. It is therefore no surprise that alternative corrosion resistant coatings that can replace cadmium have been investigated and tested by many companies and institutions all over the world.

Various alternatives are already being implemented, as for example the new A350 from Airbus has seen extensive use of Zn-Ni electroplating as a substitute, while SAAB has successfully replaced 72% of the cadmium coated lower strength steel components (UTS < 1250 MPa) on the JAS 39 Gripen multipurpose fighter jet with a ZnCoFe alloy[4]. The use of these new zinc, nickel and cobalt based corrosion resistant coatings could however not be implemented on high strength steel components due to their high susceptibility to hydrogen embrittlement, coupled with the fact that zinc evolves hydrogen when corroding. Zinc being highly active, also still relies heavily on the protection of the Cr^{VI} post-treatment to pass long term corrosion tests.

Similarly the use of nickel and cobalt salts is also problematic as they have already been noted by ECHA (European Chemicals Agency) as being responsible for organ damage, respiratory difficulties and possibly cancer[1]. Nickel compounds (oxides, sulphides and inorganics) are known to be carcinogens while both metallic nickel and cobalt are currently listed as "*reasonably anticipated human carcinogens*" in the 14th Report on Carcinogens[5], with cobalt also known for having a long lasting high toxicity hazard for aquatic life[1,6,7]. The future unrestricted use of nickel and cobalt is therefore unlikely.

In order to be successful an alternative surface treatment process not only has to minimize the risk of hydrogen exposure, operate within environmental legislation, be galvanically compatible with aluminium, and have a slow rate of corrosion, but also requires a simple method of application to allow for reliable and repetitive mass production to feed into assembly lines. Previous work has already shown that aluminium based coatings, and in particular aluminium-manganese alloys hold much promise in this regard. However, the non-aqueous electrolytic deposition method used to plate this alloy proved to be unreliable, and not suitable for uniform large scale mass production[8].

The aim of this project was therefore the development of a cadmium replacement coating based on the thermal spraying of an Al-Mn alloy, and a Mn-V based post-treatment as a substitute for Cr^{VI} surface passivation. This pre-commercial proof of concept research will assist in preparing the groundwork for the second generation of environmentally friendly corrosion resistance coatings in the aviation industry. The results obtained through short term laboratory and ISO norm qualification methods are to provide a foundation for further research and possible future implementation of a fully green solution to completely remove cadmium and hexavalent chromium from the production chain.

1.2 Background

With suitable alloy additions and treatment processes aluminium can obtain mechanical strength comparable to that of some steels, for example the 7000 series with yield and tensile strengths exceeding 600 MPa[9]. With a density of only 2700 kg/m^3 (compared to 7900 kg/m^3 for steel) it is clear why it is so abundantly used for the manufacturing of components in the aircraft industry. Reboul and Baroux[9] reported that in 2011 aluminium accounted for 80 % of airplane components, but noted that this could decrease down to ~50 % in the future due to the increased use of lightweight carbon fibre based composite materials. Which indeed it has as Boeing's new 787 consists of 50 % composites by weight[10], while composite use in Airbus's newest model A350 is said to exceed 50 %[11], thereby becoming the first commercial aircraft to utilize more composites than metals in its construction.

In the construction of areas such as the wings and fuselage aluminium alloy plates and components are sometimes required to be joined using high strength steel fasteners which are not corrosion resistant and not galvanically compatible with aluminium. These steel fasteners and other larger steel components used in the landing gear for example are therefore electroplated with cadmium, which not only has excellent corrosion resistance but due to their similar corrosion potentials are also galvanically compatible with aluminium[12], thereby preventing both environmental and bimetallic corrosion of the joints. Cadmium also has a low friction coefficient providing a form of solid lubrication[12] that prevents over torqued joints from seizing up, and good tension-torque fatigue resistance which allows fasteners

to be repeatedly loosened and retightened during maintenance and repair without being damaged.

In addition to bimetallic corrosion concerns high strength steel is also very susceptible to hydrogen embrittlement. During cadmium electroplating the hydrogen content of the steel increases, but is reduced afterwards by for example baking the components for 3-24 hours at around 200°C[13]. However, during service hydrogen can also be generated through the reduction of water when a protective surface coating corrodes, causing re-embrittlement of the steel substrate which can lead to its failure. Tests have shown that even hydrogen resistant steel such as AerMet100 that picks up almost no hydrogen during aqueous electroplating, is still susceptible to hydrogen re-embrittlement when its ED Zn-Ni coating was corroded[13].

This risk of hydrogen re-embrittlement is strongly influenced by the corrosion potential of the coating, among other factors, and is another region in which cadmium excels in protecting steel. For example, Figueroa and Robinson[13] demonstrated that a typical acid plated coating of Zn-14%Ni with a -1050mV (SCE) corrosion potential is expected to produce 100 times more hydrogen during corrosion when compared to an aluminium sol-gel coating with a potential of -800mV (SCE), which is close to the corrosion potential of ED cadmium (-750 mV)[14,15]. Pure aluminium and ED Al-Mn coatings does not have this risk of excessive in-service hydrogen evolution, and is thus well suited for use on high strength steel components. Using thermal spraying as the application method has an added advantage in that it also eliminates the 3-24 hours post application hydrogen removal heat treatment.

Economically electroplating is a low cost process that is easy to apply and repair, while many suggested alternative processes rely on newly developed proprietary technologies that can be expensive and difficult to deploy on a large scale. Therefore it is not only performance issues and material characteristics that needs to be overcome but also cost and logistical concerns in order to find and implement a practical alternative to cadmium plating[2].

However, it should also be noted that the cadmium electroplating is the last line of defence of a multi-layered system, which may consist of a chromate conversion or phosphatized coat, followed by paint (base coat and/or top coat) and other additional layers for sealing and waterproofing such as lacquers[16]. Unfortunately, in contrast to all its favourable properties cadmium is also extremely toxic, with carcinogenic, mutagenic and teratogenic effects[1,2,17,18]. Regardless of the significant risks involved, cadmium had in the past been long exempt from regulations for lack of a suitable alternative. It has now been over 40 years since the dangers of cadmium was first discovered in the 1970's after which feasible substitutes have been sought[16]. Its use in most industrial applications have now largely been banned in Europe[19] with only a

few exemptions such as the aviation industry where suitable replacements have yet to be found.

More recently under the ever increasing pressure of environmental regulations and disposal costs many new materials and deposition processes have been trialed and tested but with mixed results. The majority of successful implementations were achieved for low strength steels only. Under the European Chemical Agency's REACh legislation the year 2016 is to be the sunset year for the use of cadmium and its cyanide plating baths, requiring its replacement by "green" solutions, as after 2016 new regulations will be implemented allowing the use thereof only under severe restrictions[1,3].

In the U.S.A. the Agency for Toxic Substances and Disease Registry (ATSDR) estimates that more than 500 000 workers are exposed to cadmium every year. The primary route of exposure is the inhalation of dust and fumes, followed by the accidental ingestion of dust from contaminated hands, food and cigarettes. The workers having the highest risk of exposure are those in the electroplating and metal machining industries[6]. In Europe the electroplating of cadmium is nowadays a very small market with an estimated 20 SME coaters and some in-house platers currently in operation[3]. Due to stringent regulations the applications for electroplated cadmium have become limited to the aerospace, military and offshore industries. However in spite of this small market in Europe, the exceptional properties of cadmium have allowed it until now to remain indispensable[3].

The aim of this investigation follows the on-going trend of trying to replace aqueous processes such as electroplating with "dry" processes like thermal spraying and vacuum deposition to reduce hydrogen embrittlement concerns[2]. Using atmospheric plasma spraying to apply an aluminium alloy layer onto high strength steel will provide a less noble corrosion resistant sacrificial coating, which is galvanically compatible with aluminium and does not require a hydrogen reducing heat treatment. Previous work has already shown that pure ED aluminium coatings have poor lubricity, but that alloying with manganese improved this[2]. The presence of manganese also increases the corrosion potential of the alloy moving it closer to that of cadmium, and has shown comparable levels of corrosion resistance during neutral salt spray testing[17].

1.3 Cadmium Alternatives

Even though health, safety and environmental legislation are different in most countries, it shares the common goal of reducing cadmium usage and eventually its complete ban[2]. Since cadmium coated components carry their toxicity risks with them throughout their life cycles creating hazardous conditions anywhere they are treated, stripped, repaired or handled, the interest in its reduction is shared globally.

When considering the galvanic series of metals, aluminium and zinc are the only practical options that are less noble than cadmium and low alloy steel.
In addition to providing galvanic protection the other basic requirements for any proposed alternative coating is that it should provide an adequate level of corrosion resistance and be galvanically compatible with aluminium alloys as they are used extensively in aircraft structures. The small difference in the open circuit potentials (OCP V(SCE)) of low alloy steel (~ -0,6V)[20] and cadmium (~ -0,75V)[14,15] is one of the reasons why the combination works so well. In contrast to this zinc (~ -1,0V)[20] and aluminium (~-0,95V)[21] in contact with steel has a much higher driving force to corrode and are often alloyed to reduce this potential difference.

ED zinc alternatives that have been investigated have included pure zinc coatings as well as coatings alloyed with nickel, cobalt and tin. However, zinc based coatings have several disadvantages, they are (with the exception of Zn-Sn) not galvanically compatible with aluminium, generate a lot of hydrogen during electroplating and in-service corrosion, and are still heavily dependent on the additional hexavalent chromate conversion coating (CCC) of the surface in order to survive long term corrosion tests[2,13,15].

Any new alloy and method combination will have its own range of advantages and limitations which will be evaluated not only for corrosion resistance but various other requirements such as paint adhesion, ease of repair, torque-tension characteristics, bend-to-break, and behaviour in contact with airplane fluids such as fuels, oils and runway de-icing chemicals to name but a few[2]. Therefore the task of finding a suitable all-round replacement for cadmium is quite challenging and will most likely consist of a range of solutions, each best suited for a specific region, substrate or component.

1.3.1 Al-Mn plating in a molten salt bath

To specifically target applications where other coating technologies were unsuccessful in replacing cadmium Kane et al.[17] evaluated aluminium-manganese electrodeposited from a molten salt bath under an inert atmosphere as an anti-corrosion coating for the American Department of Defence (DoD), prior to the construction of a production scale molten salt electroplating plant. This was done not only to comply with more stringent health, safety and environment (SHE) regulations and their implementation costs, but also to reduce the potential risk of legal liability from exposing the workforce to highly toxic cadmium.

Table 1-1: Molten salt bath chemistry.[17]

Anhydrous aluminium chloride	79 mass %
Anhydrous manganese chloride	1 mass %
Sodium chloride	10 mass %
Potassium chloride	10 mass %

Combined with a Cr^{VI} post treatment these ED plated aluminium alloys, containing 15 mass % Mn, exceeded 3000 hours of ASTM B117 neutral salt spray corrosion testing, while scribed samples lasted for 2100 hours without rust formation, indicating exceptional barrier and sacrificial properties[17]. The ED coatings showed great promise when done on a small scale, but the process could not be scaled up successfully to production level[8]. The problems experienced included reproducibility and HCl fumes, as well as corrosion of process components by the aggressive molten salt electrolyte. The sensitivity of the molten salt electrolyte to moisture pickup was also a source of concern as it influenced the plating efficiency, while the formation of hydrogen chloride during the post treatment rinsing stages may also lead to hydrogen embrittlement of high strength steels, and therefore the electroplated components still required baking after processing[8].

1.3.2 Thermal spraying of Al-Mn

Thermal spraying of pure aluminium and its alloys is a flexible and inexpensive process well suited for coating larger components where coating thicknesses are allowed to exceed approximately 100 µm. Automated control of the spray gun ensures that even, uniform coatings can be obtained repeatedly, but are not suited for small components with tight tolerances such as threaded fasteners, or for coating internal surfaces. However thermal spraying of an aluminium based alloy is considerably less complicated than non-aqueous electroplating, with a fast deposition rate and no risk of hydrogen embrittlement, making it well suited for coating larger steel components. The corrosion potential of an aluminium-manganese alloy relative to that of steel makes it a worthwhile alternative to consider for replacing cadmium. In addition these alloys are also galvanically compatible with other aluminium alloys and unlike zinc does not have any in-service re-embrittlement issues.

Potentiometric testing has already shown that compared to pure aluminium, alloying with manganese leads to an increase in both surface passivation and corrosion potential while decreasing the corrosion current density of the alloy[21]. However, as the corrosion resistance of the alloy increases with manganese content, its ability to provide cathodic protection to a steel substrate decreases. Therefore when developing a new Al-Mn corrosion resistant coating alloy, the positive and negative contributions of each metal must be finely balanced in order to obtain the desired synergistic effect. Since the ED Al-Mn has shown exceptional corrosion performance, with the only drawback being the method of application, it seems opportune to also evaluate the performance of this alloy produced using different methods of application.

1.4 Toxicological evaluation

Cadmium is well known to be an extremely hazardous substance that poses a significant health risk to workers, as any inhaled fumes or dust is easily absorbed into human organ tissue and it takes approximately 30 years for the human body to expel half of the absorbed dose[17]. Exposure to cadmium is therefore highly regulated and the Occupational Safety and Health Administration (OSHA) have determined that the maximum permissible exposure limit (PEL) for workers on an 8 hour shift is only 0,005[6] mg/m^3.

As potential alternatives, aluminium and manganese are significantly less hazardous to workers and the environment, but inhalation and ingestion of their fumes and dust can still be harmful if the required personal protective equipment is not used. In the powdered form both can cause skin and eye irritation, while repeated or prolonged exposure to manganese can lead to central nervous system damage.[22,23] Expulsion of manganese from the human body does however occur relatively fast, as half the dose is eliminated after 37 days[17]. The greatest risk of Al-Mn coated components will most likely be exposure to dust when grinding the material as the OSHA PEL of 15 ppm and 5 ppm limits in air for aluminium and manganese respectively might be exceeded[6]. Overall the toxicity of the alloy is very low with tests on rats and rabbits using a 70:30 Al:Mn powder indicating that the LD_{50} is greater than 2 000 mg/kg body weight, and is also evident in the fact that the 3003 series Al-Mn alloy is commonly used for manufacturing beverage cans and cookware[17].

From an entire life cycle perspective the costs associated with the cadmium coating process account for only part of the total cost of compliance with SHE regulations. The in-service costs are accumulated through the unavoidable generation of hazardous waste during maintenance. For example cadmium dust is generated during cutting and grinding of seized bolts or mechanical stripping, while chemical stripping generates large volumes of hazardous waste. Even rinse water of equipment containing cadmium coated parts has been reported to be contaminated with Cd[17]. The cost for collection, treatment and disposal of these hazardous in-service wastes are high, and the risk of exposing labourers to even small quantities of cadmium dust or fumes which exceed the OSHA limits can result in significant legal and medical costs. Therefore even if the initial equipment and processing cost of new alternative coatings might initially be more expensive than cadmium electroplating, it can still be much more economical over the entire component life cycle if a lack or reduction in toxicity can provide significant environmental health and safety benefits[17].

1.5 Solidification of Al-Mn

Previous investigations of ED Al-Mn have revealed a strong connection between the microstructure of the alloy and its corrosion resistance[24]. The Al-Mn binary system is very complex, and once the ~2 mass % solid solubility limit of manganese in aluminium is exceeded the formation of various intermetallic phases such as Al_6Mn, Al_4Mn and $Al_{11}Mn$ can be expected under equilibrium cooling conditions. For corrosion resistance their presence would present a problem as these intermetallic compounds are more noble than the surrounding matrix, and can compromise the effectiveness of the alloy. It has been noted however that the Al-Mn binary phase diagram is not an accurate representation for metastable thin films[25].

The reported microstructures for ED Al-Mn from a molten salt solution has been supersaturated FCC aluminium at low concentrations of manganese, and an amorphous phase close to Al_4Mn in composition for higher concentrations[26,27]. If applied as a corrosion resistant coating the supersaturated FCC microstructure is desired and have been achieved for deposits containing up to 18 mass % manganese[21,28]. Adding more manganese than this results in the formation of a mixed microstructure containing both the supersaturated and an amorphous phase, up to around 45 mass % manganese at which point only the amorphous phase is present[21].

During plasma spraying, very high cooling rates in the order of 50 000°C per second[29] can be reached which allows the maximum solid solubility limit to be exceeded by quite a large margin, resulting in the formation of supersaturated metastable phases. Theoretically therefore the extremely fast cooling rate experienced by an atmospheric plasma sprayed Al-Mn coating should allow the formation of a single uniform supersaturated aluminium layer within the 10 - 20 mass % Mn range, and avoid the formation of unwanted secondary phases. The risk of using atmospheric plasma spraying to apply an Al-Mn coating is that not all feed particles will follow the same trajectory through the plasma plume, with some being fully melted, others partially melted and some remaining unmolten. If therefore there are any unwanted intermetallic phases present in the feed powder these can still be carried over into the coating itself.

The other major risk of using a supersaturated coating is that when it is exposed to high temperatures some intermetallic phases can start forming. In addition to this aluminium can also start reacting with the steel substrate forming the hard and brittle Fe_2Al_5 intermetallic at the interface[30]. Therefore similar to ED cadmium coatings which are limited to a maximum in-service temperature of 235°C, thermally sprayed Al-Mn alloys would also need to be restricted for use in high temperature regions of the aircraft.

1.6 Atmospheric Plasma Spraying

Atmospheric plasma spraying (APS) is one of the thermal spraying processes utilized for the application of protective coatings onto a substrate material, and remains one of the most widely used processes compared to other alternative coating methods such as chemical vapour deposition (CVD), sol-gel, physical vapour deposition (PVD) and plasma electrolytic oxidation (PEO)[31]. It is popular as it does not damage the substrate, has a low operating cost and high processing speed that allows thick coatings to be deposited at a fast rate[29,32]. A feeder injects metallic powder at one or more positions into the plasma arc, where it is molten and accelerated towards the target by a carrier gas such as nitrogen or argon. The technology is already well established and production can be automated for a very wide range of external applications onto components of almost any size or geometry.

For each application the process parameters and material must be individually optimized to obtain the best results. There are however numerous fluctuating parameters involved in the plasma spraying process such as the arc instability caused by voltage fluctuations and powder feed rates that can lead to poor reproducibility of results, and has had a negative influence on the industrial development of the process[33,34]. Studies by Bisson et al.[35] on particle fluctuation parameters and plasma plume length by Kieschke et al.[36] revealed particle temperature and speed fluctuations of up to 600 ºC and 200 m/s, and plasma jet length fluctuation of 200 mm respectively.

Differences in the particle size distribution of the feed powder will affect the pneumatic conveying characteristics within the carrier gas and through bends in the feed tube, which influences the trajectory and residence time within the plasma plume[33]. Varying the processing parameters such as the carrier gas flow rate, powder feed rate and angle of injection etc. creates different particle splat patterns and sizes[37] resulting in significant change in the final porosity and overall quality of the coating. Great emphasis must also be placed on the adhesion of the coating to the substrate of the component under operating conditions. Surface preparation is therefore critical, and components should ideally be sand blasted for roughness and be free from any contaminants such as oil, water or oxidation before coating[38]. Some of the drawbacks of APS compared to ED coating is the minimum thickness of the coating that can be applied, which makes it unsuitable to coat tight tolerance components such as threaded fasteners, its inability to coat internal surfaces and the rough outer surface it creates typically requires shot-peening to smooth out.

For corrosion resistance the performance of the coating not only depends on the composition of the alloy but also on the quality of the coating structure. The repeated deposition of flattening particles or splats 1 - 2.5 µm[38] thick and roughly 60 µm[38] in diameter gives APS coatings their typical lamellar and pore like structure. Porosity plays a prominent role in the corrosion resistance of the coatings as incomplete

bonding between splat lamellae allows a pathway for electrolyte from an aggressive solution to reach the substrate. The porosity of the applied coating therefore needs to be minimized through the optimization of combined sets of processing parameters. The seven types of porosity occurring in thermally sprayed coatings have been identified by Vreijling[39] as stacking porosity, gas pockets, evolved bubbles, splat disintegration, partially evaporated particles, micro cracks and shrinkage pores. For the improvement of the corrosion resistant properties post-treatments such as laser glazing, cold pressing and hot pressing have been used for densification, or sealants such as epoxies, polyurethanes, phenolics and silicones can also be used to seal off the pores[40].

Previous attempts at using non-aqueous ED Al-Mn plating to replace cadmium on high strength steel aircraft components proved that this alloy can indeed provide an excellent level of corrosion resistance[17]. The ultimate downfall of the process that prevented its industrial implementation was the difficulty of operating the molten salt plating bath on a large scale[8]. The Al-Mn alloy itself performed admirably and when treated with hexavalent chromium, showed a level of corrosion resistance comparable to that of cadmium[17]. By using atmospheric plasma spraying to apply this alloy as a corrosion resistant layer the difficulties associated with of non-aqueous electroplating can be avoided, and might still allow Al-Mn alloys to replace cadmium on large steel components.

1.7 Corrosion of aluminium

Like stainless steel pure aluminium is a passive metal in natural environments but, its mechanical strength is however poor, and unlike stainless steel it does not require alloying for corrosion resistance but rather for increased mechanical properties. When exposed to oxygen bare aluminium reacts within milliseconds to form an amorphous oxide film 2 - 4 nm thick which significantly reduces further oxidation. Considering the Pourbaix diagram for aluminium it follows that this Al_2O_3 oxide film should remain intact in neutral environments, but in more basic or acidic conditions, i.e. when the pH value increases above 9 or below 4, its corrosive protection is lost[9,14]. The Al_2O_3 film hydrolyses in humid environments to form aluminium oxyhydroxide AlOOH:H_2O which offers less protection than the original oxide layer. However as it has a higher volume than the oxide it tends to fill surface irregularities and the large number of pores and micro defects present in the original oxide layer, thereby reducing the number of favourable initiation sites for pitting corrosion[9].

Corrosion pits in chloride containing environments are typically initiated at localized weak points in the oxide layer where micro defects, impurities or intermetallic compounds are present. However not all the pits initiated at the surface will propagate as the corrosion mechanism is controlled by the cathodic reaction[9]. When pure unalloyed aluminium comes into contact with chloride and a suitable oxidant such as dissolved oxygen, it has been reported by Reboul et al.[41] that the initial

number of pits formed is in the range of ~10^4/cm^2, while Warner and Schmidt[42] found an increase of two orders of magnitude for copper containing AA2024 (~10^6/cm^2) which is one of the aluminium alloys used extensively in the aviation industry. Once initiated pit growth occurs through the following auto catalytic reactions[43]

Dissolution of Bayerite film:

$$\boldsymbol{Al(OH)_3 + Cl^- \rightarrow Al(OH)_2Cl + OH^-} \quad 1.1$$

Attack of chloride ion on the aluminium substrate:

$$\boldsymbol{Al + 4Cl^- \rightarrow AlCl_4^- + 3e^-} \quad 1.2$$

Regeneration of the chloride ions (Aggressive solution in capped pit)

$$\boldsymbol{AlCl_4^- + 3H_2O \rightarrow Al(OH)_3 + H^+ + 4Cl^-} \quad 1.3$$

The mobile Cl^- anions build up inside the pits because they are mainly responsible for the current transport which leads to their increased localized concentration and the formation of the $AlCl_4^-$ - complex from equation 1.2 at the interface, gradually increasing the pit depth. The hydroxide formation in equation 1.3 generally occurs on the lip of the pit opening where the bulk pH value is close to neutral, resulting in the gradual build up and formation of a white alumina cap over the pit. The cap partially or completely seals off the pit helping to maintain its corrosive activity by restricting the dilution of the protons and chloride ions being generated, which leads to the build-up of an aggressive corrosive solution inside the pit[9].

The propagation of the pits are stopped either when the corrosion current decreases to such an extent that the $AlCl_4^-$ complex layer formation is no longer occurring fast enough anymore, allowing it to be replaced again by the passivating oxide film[43]. Or, alternatively, when the evolution of H_2 gas builds up to such an extent that it ruptures the capped off pit, expelling and diluting the corrosive electrolyte[9,43]. During neutral salt spray (NSS) testing, pitting corrosion is the mechanism responsible for the failure of aluminium samples. Electrochemical measurements have already indicated that alloying aluminium with manganese leads to improved surface corrosion resistance[21]. If the presence of manganese is also capable of impeding or influencing the corrosion mechanism responsible for pit formation, it would result in a significant increase in the survivability of aluminium in an aqueous chloride environment.

2 Surface Passivation

2.1 Chromate Conversion Coating (CCC)

Aluminium alloys used in the aerospace industry whether thin 2024 plates or thicker 7075 machined components are always subjected to one of two surface passivating processes, either anodizing or conversion coating (Figure 2.1-1). Both of these processes traditionally utilize the very effective properties of the hexavalent chromium ion. During chromic acid anodizing (CAA) the ions are entrapped within the 5 - 7 µm thick honeycomb like oxide layer, and during chromate conversion coating the Cr^{VI} ions are retained on the thin film that forms on the surface. Of the two methods, the anodizing process has seen the very successful large scale industrial implementation of sulphuric acid anodizing, typically in combination with an organic acid (tartaric sulphuric acid (TSA) anodizing is used by Airbus, and boric sulphuric acid anodizing (BSAA) by Boeing). The same successful large scale implementation of a dominant CCC replacement within the industry has however not yet been achieved, with the widespread use of chromate conversion coatings still remaining commonplace.

As hexavalent chromium is an active constituent in the coating baths, the primary film forming agent and corrosion inhibitor, there is a great demand reinforced by environmental, health and safety legislation to completely phase out its use[44]. Research and development of chromate free processes are on-going but the excellent performance and ease of application have ensured its continued use, especially in high demand applications[45].

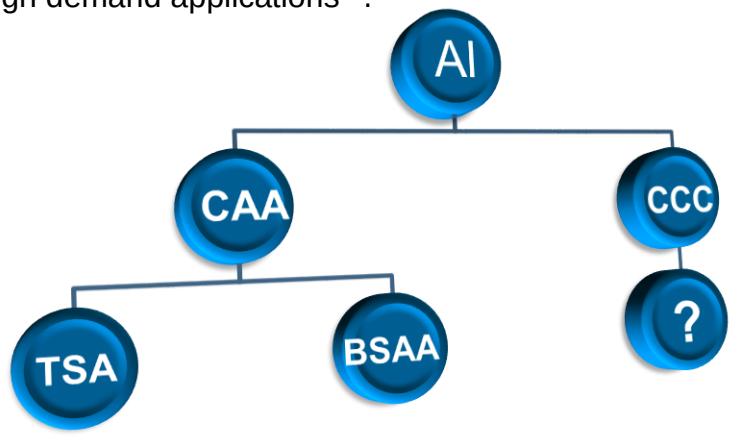

Figure 2.1-1: Illustration of the older Cr^{VI} based surface passivating processes used for aluminium, and the next generation of green replacements.

The term “conversion coating” refers to the chemical conversion of the surface of a metal component to improve the adhesion of paints, while also acting as a secondary corrosion resistant layer. The application of a chromate conversion coating is not a single process, but rather a series of processing steps, generally consisting of cleaning(s), de-oxidation, conversion coating, and drying. In between each stage of the sequence there is typically also a drag rinse and final rinse of

components, which may include water-break tests to assess the surface condition if required by the manufacturing specification.

Unlike chromic acid anodizing which utilizes current flow to build up an oxide layer 5-7 µm thick, chromate conversion coatings form spontaneously during contact with the substrate without the need to apply any current or voltage, and is typically ~0.3 µm[45,46] thick after about 3 minutes of submersion. The coatings are commonly applied to aluminium but also onto zinc, magnesium, cadmium, tin and iron based alloys for the primary purpose of either improving adhesion of paints or improving the corrosion resistance of the active substrates.

Film formation on the aluminium substrate is initiated by the reduction of Cr^{VI} to Cr^{III} in a series of reactions, which leads to an inorganic polymer $Cr(OH)_3$ structure known as the "backbone" of the coating[47]. After approximately 30 seconds the growth of the film slows down[48], or stops[49] but the ratio of Cr^{VI} to Cr^{III} continues to increase as the Cr^{VI} is adsorbed onto the structure through the nucleophilic attack of hydroxyl ligands resulting in Cr^{III}-O-Cr^{VI} linkages. After commercial treatment times Cr^{VI} ions typically account for 20 - 40% of the total chromium content of the coating[45].

Probably the best known property of chromate conversion coatings are their self-healing ability which results from the coating's ability to store Cr^{VI} ions, and releasing them at chemical or mechanical defect initiation sites where they are reduced to form insoluble Cr^{III} hydroxide to counteract the damage[50]. The Cr^{VI} ions are released through diffusion controlled transport, and have been proposed to occur by the following reaction[51]:

$$\boldsymbol{Cr^{3+}\cdots O\cdots Cr^{6+}}(s) + \boldsymbol{H_2O} \leftrightarrow \boldsymbol{Cr^{3+}\cdots OH} + \boldsymbol{Cr^{6+}}(aq) + \boldsymbol{H^{+}}(aq) \qquad 2.1$$

The Cr^{VI} content of a chromate conversion coating slowly diminishes and will eventually disappear during exposure to a corrosive environment[52]. Initially chromate conversion coatings are amorphous and gel-like when fresh, but harden during dehydration, forming shrinkage cracks as the coating dries out giving it its characteristic mud-cracked appearance. To obtain good adhesion it is necessary to paint components within the first 24 hours after application; similarly if the coating is to be subjected to a corrosion test without a top coat it must also be allowed to dry for at least 24 hours beforehand[53].

Eventhough these chromate coatings are very thin with a mud-cracked surface structure they impart excellent corrosion resistance and can easily double or tripple the time to failure of samples during NSS testing. This not only applies to aluminium but also ED alloys and has for example been shown that Sn-Zn coated samples that lasted for around 400-600 hours in the salt spray chamber without a surface treatment, would last a minimum of 1200 hours after a CCC treatment[54].

This clearly illustrates the significant increase in corrosion resistance this quick, simple and cost effective dipping operation brings to the fore, and why it is so commonly applied to aluminium components.

2.2 Chromate free conversion coatings

In 2007 RoHS regulations limiting the use of hexavalent chromium came into effect restricting the chromate content in conversion coatings to 0.1%[44], as it was classified as a Substance of Very High Concern (SVHC), and might possibly be completely forbidden in the European Community by 2017[55], necessitating the development and implementation of new chromate free conversion coatings. New conversion coating alternatives are based on elements with chemical behaviour either closely resembling that of chromium, or elements that possess multiple oxidation states, which can potentially provide active corrosion protection (Figure 2.2-1). Numerous investigations for replacement coatings have been undertaken with proposed alternative coatings including permanganate, trivalent chromium, cerium, titanium-zirconia, vanadium, molybdenum and sol-gel methods or combinations of these compounds[45,55,59,61].

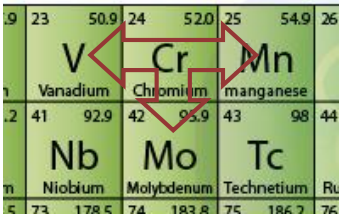

Figure 2.2-1: Elements surrounding chromium in the transition metal section of the periodic table.

Each of these proposed alternatives have their own processing and performance ranges and might be suitable for some industries but not for others. The aerospace industry falls into the high performance market and the extremely strict safety standards maintained requires excellent stand-alone performance of unpainted conversion coatings in the salt-spray test, preferably also with a drop-in application method that would not require major modifications to already existing processing facilities[45]. Before trying to develop a new chromium free surface treatment for aluminium it is important to know what other alternatives has already been investigated; below is a closer look at some of the other proposed solutions.

2.2.1 Trivalent Chromium Conversion Coating

Trivalent chromium based solutions have seen increasing interest as a possible replacement for CCC, but have yet to gain wide spread commercial use. Trivalent chromium conversion coatings provide good adhesion for paints and offer barrier protection in the form of Cr^{III} oxide and hydroxide compounds, but do not process the self-healing ability of the hexavalent coatings and are therefore generally combined with zirconia. It has been reported that despite the absence of Cr^{VI} in the coating baths, up to 1% Cr^{VI} are still found in coatings after ambient ageing or after sodium

chloride based corrosion tests. It has been suggested that the generation of hydrogen peroxide produced during the reduction of dissolved oxygen is responsible for oxidizing Cr^{III} to Cr^{VI}.[55,62]

2.2.2 Permanganate based conversion coating (PCC)

Manganese follows chromium in the transition metals section of the periodic table, sharing many chemical similarities with chromium, therefore heptavalent manganese (Mn^{VII}) has been a logical choice for trying to mimic the success of hexavalent chromium in reducing from a higher valence state to a lower valence oxide during corrosion. The difference being that Mn^{VII} in its common form of potassium permanganate ($KMnO_4$) is not toxic or hazardous, while manganese based conversion coatings have been claimed by some reports to have nearly equivalent corrosion protection to traditional chromate based coatings[44,63].

Potassium permanganate based coatings have already found some application in industry with patented processes existing for a variety of aluminium alloys[64]. During the application of permanganate conversion coatings Mn^{VII} acts as the oxidizing agent and produces MnO_2 or Mn_2O_3 oxide layers on the substrate[65]. The proposed mechanism being the reduction of Mn^{VII} to Mn^{IV} as MnO_2 (Equation 2.2), the majority of which then becomes hydrated.

$$\boldsymbol{Al + MnO_4^- + 2H_2O = Al(OH)_4^- + MnO_2} \qquad 2.2$$

The formation of these oxide surface layers are known not to provide good protection at lower pH values, but does inhibit surface corrosion at higher pH levels. Whether any amount of Mn^{VII} ions are retained in the coating seems uncertain as some publications have reported that their permanganate conversion coatings contained no MnO_4^- ions[41] while other authors have reported MnO_4^- accounting for ~ 22% of the manganese in their conversion coatings[61].

In terms of corrosion resistance PCC provides a good alternative for CCC, the major problem preventing its wide spread industrial implementation is the instability of the bath pH. The reduction of Mn^{VII} to a lower state results in the consumption of H^+ from the solution and a subsequent increase in pH. In HCl containing baths $Na_2B_4O_7$ has been found to provide the required buffering effect for the bath. However, disodium tetraborate is a highly toxic substance it has also been listed as a Substance of Very High Concern (SVHC) in REACh legislation and its use will likely soon be forbidden[55].

2.2.3 Vanadium based conversion coatings

Vanadium based conversion coatings seems to be one of the most promising alternatives for replacing the CCC process, as it reacts readily with the surface of active metals to form a protective passive layer. The coating consist mainly of the oxides and hydroxides of V^{V} and V^{IV}, and similar to CCC have been reported to process a self-healing ability, allowing corrosion initiation sites such as cracks or pits to be repaired[55]. While polarization measurements have shown that a vanadate coating can obtain a corrosion potential very similar to that of traditional chromate coatings[60]. The following mechanism has been proposed to explain the functioning of a vanadate conversion coating. Initially the vanadium (V^{V}) in solution hydrolyses on the component surface according to equation 2.3[60]:

$$\boldsymbol{VO_2^+ + 2H_2O \rightarrow VO(OH)_3 + H^+} \qquad 2.3$$

During contact with a corrosive medium the coordination number of the hydroxide changes from that of a tetrahedral structure to octahedral through the addition of two water molecules. Polymerization of the octahedral structure through the formation of V^{V}-V^{V} and V^{V}-V^{IV} linkages results in the formation of a new protective barrier layer[66].

2.2.4 Molybdenum based conversion coatings

Molybdenum has been considered as another possible chromate replacement, and can be added to the conversion solution in the form of molybdate oxyanions such as sodium- or ammonium molybdate. It was found by Wang et al.[67] that molybdate conversion coatings performed better on a Mg-Li alloy when combined with $KMnO_4$. Similarly Yoganandan et al.[61] recently also obtained excellent corrosion resistance using the permanganate-molybdate combination for a conversion coating on aerospace grade 2024 aluminium. In much the same way as hexavalent chromium, present as CrO_4^{2-}, both these metals are multivalent and could possibly mimic the self-healing ability of Cr^{VI} if they can be retained in their ionic states such as MnO_4^- or MoO_4^{2-} to improve corrosion resistance by repelling charged Cl^- ions or being reduced to stable oxides whenever the barrier coating is compromised[61].

Polarization tests further revealed that the coating improved pit growth resistance, and when applied to a sulphuric acid anodized 2024 plate it successfully passed 1000 hours of salt fog exposure. Measurements taken throughout the test showed a continuous decrease in both the manganese and molybdenum concentrations of the surface layer, possibly indicating their active involvement in providing long term corrosion protection, exhibiting similar behaviour to that of hexavalent chromium in a corrosive environment[61].

2.2.5 Titanium and zirconium

Titanium and zirconium based conversion coatings have a well established market and has been used in various industries including on aluminium and titanium components in fighter jets and the AA2219 alloy of NASA's solid rocket boosters and can be applied relatively simply in a 5-8 stage process e.g. alkaline clean, rinse, coat, rinse and dry[45,68].

The bath solution used is acidic and generally contains the hexafluoro metal complexes H_2ZrF_6 and H_2TiF_6 and a polymer such as polyacrylic acid[69] or phenolic resins[70] for improved corrosion resistance. It has been reported that these coatings have excellent adhesion properties, but requires long treatment times of ~20 minutes while the coatings produced are generally very thin, typically only 10-25 nm and quite porous which results in poor corrosion resistance when not painted[45]. Another objection to this type of coating it that it is colourless which severely limits quality control through visual inspection of components in the production line[58].

These issues were addressed recently by Yi et al.[71] through their development of a golden coloured titanium and zirconia based conversion coating, while Zuo et al.[58] successfully decreased coating times down to ~1 minute while simultaneously increasing the thickness and density of the coating by adding tannic acid and metavanadate to the bath. This modified coating consisted of various components including oxides (TiO_2, ZrO_2, V_2O_5), fluorides (AlF_3 and ZrF_4) and some metal-organic complexes[58].

2.2.6 Rare earth element based coatings

Corrosion resistant coatings based on rare earth elements such as cerium and lanthanum have also been developed and are reported to have a "scavenger effect" that inhibits the effect of minor impurities (such as chlorine and iron) through the formation of intermetallic compounds[55]. This is seen as an interesting property in line with the self-healing ability of CCC coatings. Coatings focussed on the aerospace industry are typically 100 – 400 nm thick, including the silicate based sealant, and only requires processing times of 1-2 minutes[45].

The cerium salts $CeCl_3$ and $Ce(NO_3)_3$ are typically used. Of the two $Ce(NO_3)_3$ provides a smoother and more homogenous surface, while $CeCl_3$ tend to give a surface coating with the mud-cracked appearance and also risks the entrapment of residual chloride. The chloride ions nevertheless speed up the deposition rate as they are capable of disrupting the passivating alumina layer, resulting in much faster deposition times[59]. A big drawback of using these elements is that they are expensive[55] which can render large scale industrial processing uneconomical.

3 Part A: Development of an aluminium-manganese corrosion resistant coating for high strength steels

To produce a test quantity of an atomized aluminium-manganese alloy powder suitable for atmospheric plasma spraying, the right alloy composition needed to be obtained first. Work previously done with ED AlMn alloys already indicated a loss of sacrificial protection when the manganese content exceeded 15 mass %[17]. An additional risk of adding too much manganese into the alloy is the formation of galvanically more noble intermetallic compounds which can act as localized corrosion initiation sites, while also reducing the ductility of the coating. Similarly having too little manganese in the alloy would not result in the protective coating outperforming pure aluminium, and would not justify the additional costs incurred for producing it.

The 10-15 mass % Mn range was therefore considered as the region with the optimal composition balance for possibly obtaining a level of corrosion resistance exceeding that of pure aluminium, while keeping most of the manganese in a state of solid solution. Ideally the corrosion resistance and behavioral characteristics of the entire range of Al-Mn alloys should be tested to determine the best performing composition. However, since the costs associated with creating a test quantity of atomized praying powder is very high and preceded by a three month waiting period, doing so was outside the limits of this investigation. Instead electrochemical screening and hardness measurements were used to select the best alloy composition.

Once the ideal alloy composition was known, atomization could be used to create an alloy powder with a PSD suitable for plasma spraying. The physical characteristics of the sprayed coating could still be detrimental to its performance if for example the porosity was too high. The right set of operating conditions of the equipment needed to be found through trial and error by varying the thermal spraying parameters to determine the combination that produced the densest and most homogeneous coating. The corrosion resistant properties could then be evaluated using anodic polarization measurements, laboratory scale salt bath submersion tests and ISO 9227 / ASTM B117 standardized neutral salt spray testing. The APS process has a low heat input, fast deposition rate, low operating costs and does not require a post-treatment hydrogen bake, making it highly suitable for coating tempered steel. These tests serve to provide an initial proof of concept that an Al-Mn alloy, as an environmentally friendly corrosion resistant coating, can provide a competitive level of protection when applied onto a high strength steel substrate, by using atmospheric plasma spraying as the method of application.

3.1 Electrochemical screening of Al-Mn alloys

Initial electrochemical screening tests were performed on bulk alloys prepared by melting together pure aluminium and manganese in an induction furnace with a neutral argon atmosphere. One control sample of pure aluminium and eight Al-Mn alloys containing 8 – 22 % manganese by weight were produced by heating the raw materials inside small alumina crucibles up to 1350°C (M_p Al = 660°C; M_p Mn = 1246°C) and keeping the melt at this temperature for a duration of 10 minutes, followed by slow furnace cooling. As seen in the photos below (Figure 3.1-1) the alloy samples contained some oxidation on the outer surfaces, and also some internal porosity as there is no stirring or de-oxidation of the melt inside the induction furnace, but EDX measurements confirmed that the aimed for compositions for all eight alloys were achieved.

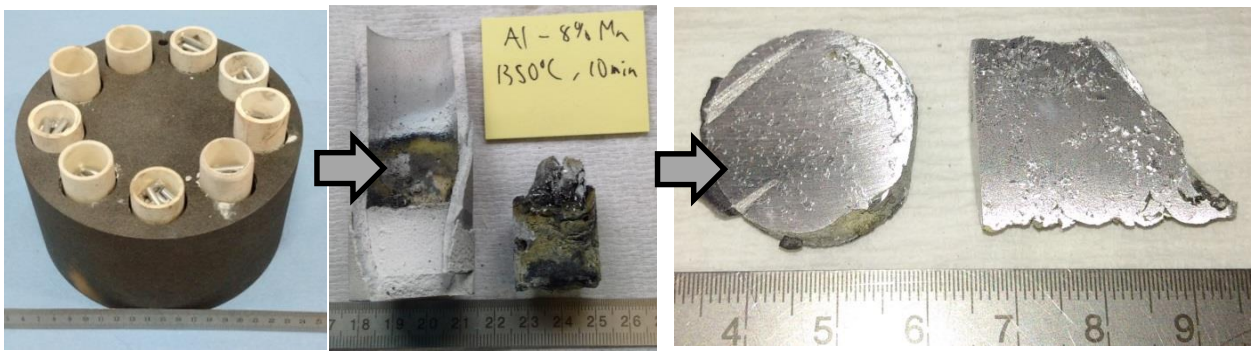

Figure 3.1-1 : Illustration of the method used to produce screening alloys of various compositions of Al and Mn by melting together raw materials in an induction furnace.

The problem with these screening alloys was that their cooling rate was considerably slower to that which the molten alloy droplets will be exposed to during APS, and would therefore consist of different phases. Unfortunately continuous cooling diagrams are not available for these alloy compositions, but looking at the Al-Mn equilibrium phase diagram (Figure 3.1-2) still gives an idea of the type of intermetallic phases that might be present in these furnace cooled samples, most likely along with various other metastable phases, as discussed in the previous section.

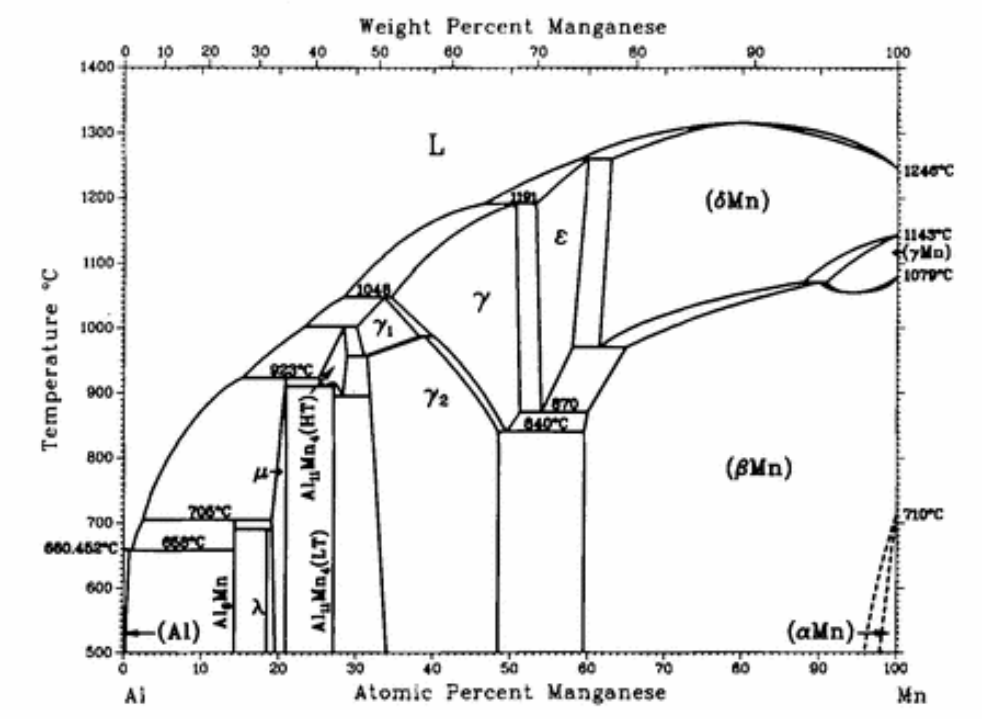

Figure 3.1-2: Aluminium-manganese binary phase diagram[73].

Once solidified the bulk alloys were sectioned using an ATA Brilliant 250E and grinded on two sides using 220 grit SiC paper to produce approximately 5mm thick coin shaped samples for polarization and open circuit potential measurements at the Ilmenau University of Technology. The potentiodynamic polarization measurements were conducted following pre-exposure of the samples to the electrolyte at open circuit, using a standard three electrode setup on a 0,13 cm^2 sample area in a 3.5 mass % NaCl solution, with a platinum counter electrode and a Ag/AgCl reference electrode in a saturated KCl solution. Polarization was initiated at -0.2 V relative to the corrosion potential in a positive direction at scan rate of 0,1 mV/s.

Figure 3.1-3 displays the polarization characteristics of the eight screening alloys, high carbon 42CrMo4 steel (EN19 / AISI 4140: 0.4 mass% C, 1.1 mass% Cr, 0.3 mass % Mo), and this steel coated with pure APS aluminium with and without a MnV conversion coating on it. Due to the impending phase changes these values only serve as an indication of each alloy's electrochemical characteristics, which was expected to improve after plasma spraying as unwanted intermetallic phases would be replaced with super saturated aluminium.

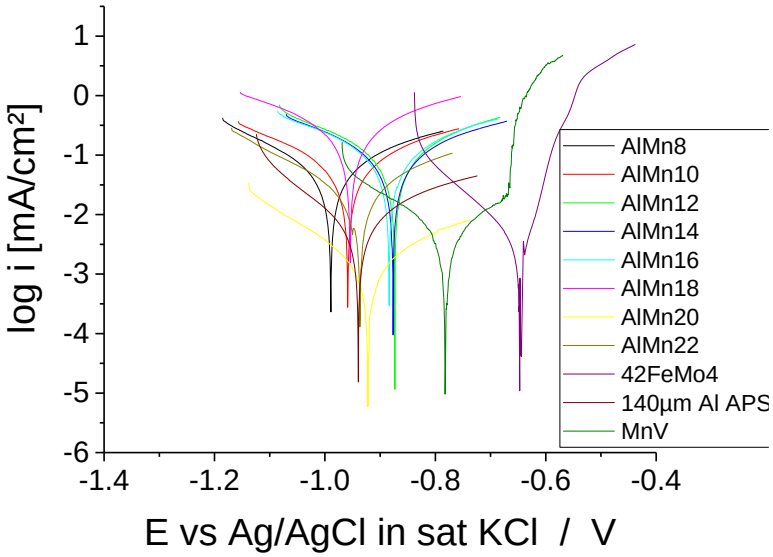

Figure 3.1-3: Potentiodynamic polarization curves obtained for the AlMn alloys in 3.5 mass % NaCl, after a pre-exposure of 25 hours.

Table 3-1: Values of samples after 25 hour anodic polarization screening.

Sample	E_{corr} (V)	i_{corr} (µA)	i_{corr} (µA/cm²)	ß$_a$ (mV)	ß$_c$ (mV)
Al	-0.940	0.884	7.04	226.1	146.2
AlMn8	-0.989	12.904	102.74	443.9	347.5
AlMn10	-0.959	18.785	149.56	550.5	492.5
AlMn12	-0.873	28.885	229.98	512.0	507.7
AlMn14	-0.876	32.499	258.75	745.6	571.2
AlMn16	-0.884	36.923	293.97	708.4	641.1
AlMn18	-0.954	114.980	915.44	939.9	829.3
AlMn20	-0.922	55.279	2.23	305.1	217.6
AlMn22	-0.936	4.001	31.86	273.3	279.9
42CrMo4	-0.647	0.196	1.56	50.7	90.3

The corrosion potential of the 42CrMo4 steel, to be used as the coating substrate later on, had a corrosion potential of -0,65 V while that of the pure APS aluminium and ED cadmium (not shown here) was measured as -0,95 V and -0,8 V respectively. Preferably the corrosion potential of the coating alloy should lie in the region between that of steel and aluminium, and with the lowest possible corrosion current density, to indicate cathodic protection for steel and a slow rate of corrosion. Of the three samples that met this criteria (12,14, and 16 mass % manganese) the 12 mass % manganese alloy was selected as it had the lowest corrosion current density.

Although at 230 µA/cm^2 its current density was still much higher than that of pure aluminium at 7 µA/cm^2, it was believed that phase changes resulting from a faster cooling rate would improve the alloy's corrosion current density. Considering that the AlMn20 alloy had the lowest corrosion current density, previous work[21] have indicated that this high quantity of manganese generally only gives the appearance of a better preforming alloy due to increased surface passivation, but at the expense of its ductility and loss of its sacrificial corrosion protection. This would likely have

resulted in a very brittle APS coating unable to pass neutral salt spray testing in the artificially damaged state.

The effect of manganese on the hardness of aluminium alloys are illustrated in figure 3.1-4 below. The graph of the hardness measurements acquired from the nine screening samples clearly shows the increased level of embrittlement when the alloy composition exceeds 18 mass % manganese. In addition to the increase in hardness and loss of cathodic protection, using a high quantity of manganese in the alloy also increases the risk of forming intermetallic compounds that can be galvanically more noble than the matrix and lead to accelerated pitting corrosion.

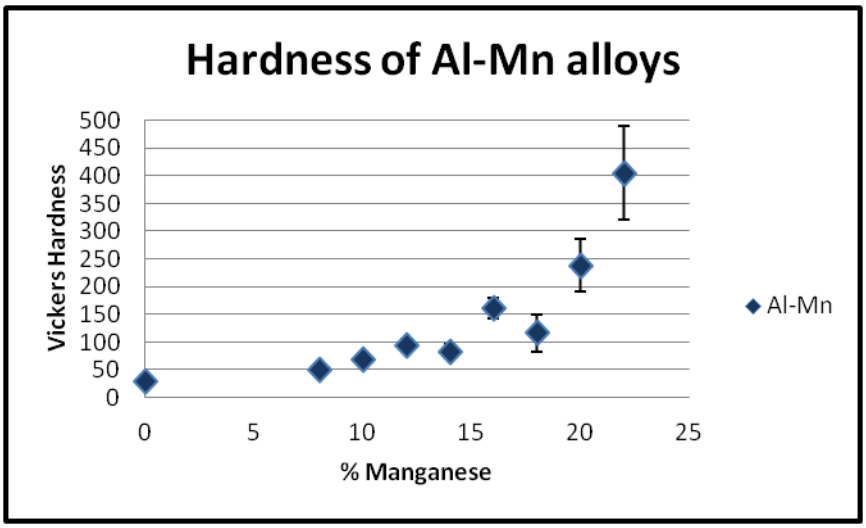

Figure 3.1-4: Influence of manganese on the hardness of the Al-Mn screening alloys.

Unfortunately these results obtained from the phases and microstructures of the furnace cooled alloys were rather poor simulations for actual APS produced coatings, but nevertheless did serve to provide an indication into the potential performance of the alloys.

3.2 Atomization of the selected AlMn12 alloy

The in-house atomization facility was used to prepare the Al-Mn alloy feed powder of the selected composition and with the desired particle size distribution. Pieces of cast aluminium and electrode manganese flakes were mixed in a 88:12 Al:Mn mass ratio, and melted in an induction furnace under a neutral argon atmosphere, shown in figure 3.2-1. Once completely molten and well mixed a stopper at the bottom of the furnace was broken off, allowing the molten metal to drip into a gas stream which dispersed the metal droplets into a mist, thereby allowing the alloy to solidify as small spherical particles. The fine powder falling to the bottom was classified into two size fractions through the use of a cyclone. The particle size distributions (PSD) measured for both the coarse and fine powder fractions obtained are indicated in Figure 3.2-2.

Figure 3.2-1: Tundish with stopper inside the induction furnace on the left and classification cyclone on the right.

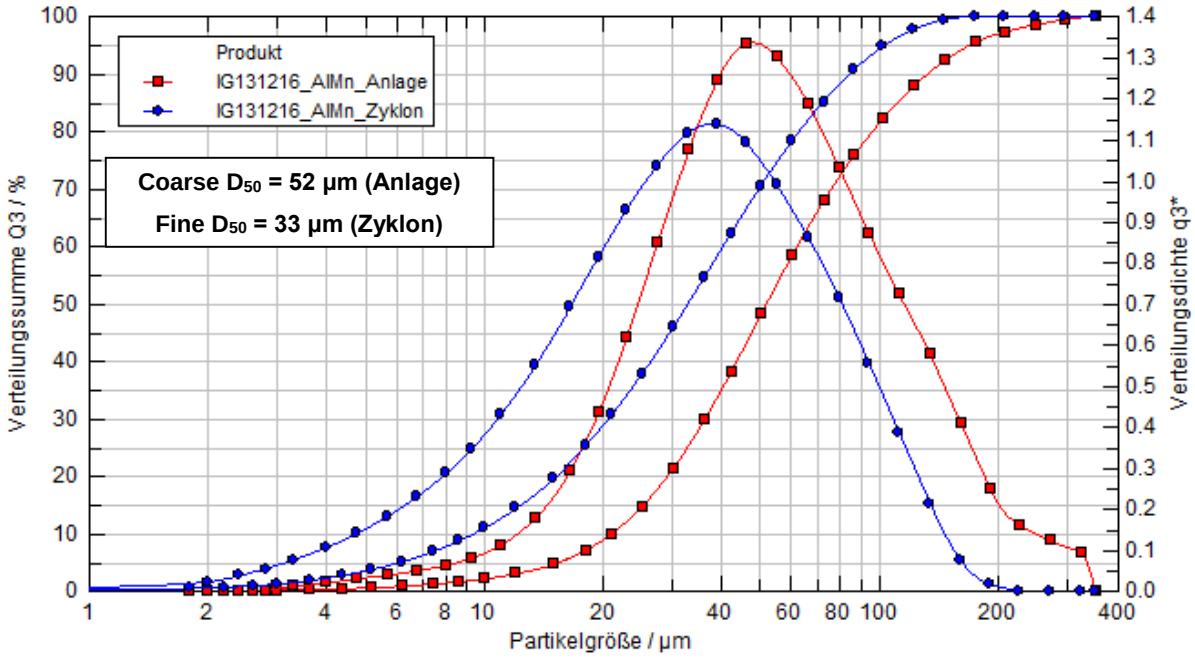

Figure 3.2-2: Particle size distribution of the coarse and fine sections of the obtained AlMn12 powder.

The coarser fraction of the two powders was selected to use as the APS feed, as its size range allows more momentum to be imparted to the particles for a better trajectory into the plasma plume. Before using it the feed powder PSD was further refined through mechanical sieving to remove the over size (+90 µm) and under size (-32 µm) fractions to facilitate the production of a more homogeneous alloy coating. The nature and distribution of the unscreened coarse fraction of the atomized AlMn12 alloy are illustrated in the secondary electron image shown as figure 3.2-3. When looking at the larger particles it appeared as if some secondary phase transformation might have occurred after solidification of the droplets. This is not unexpected as the solubility of manganese in aluminium is only ~1.8 mass %. At a

manganese content of 12 mass % the thermodynamic driving forces for the formation of intermetallic compounds would be exceedingly high and the residual heat after solidification or possibly ambient temperature seems to allow sufficient diffusion for some phase change to take place.

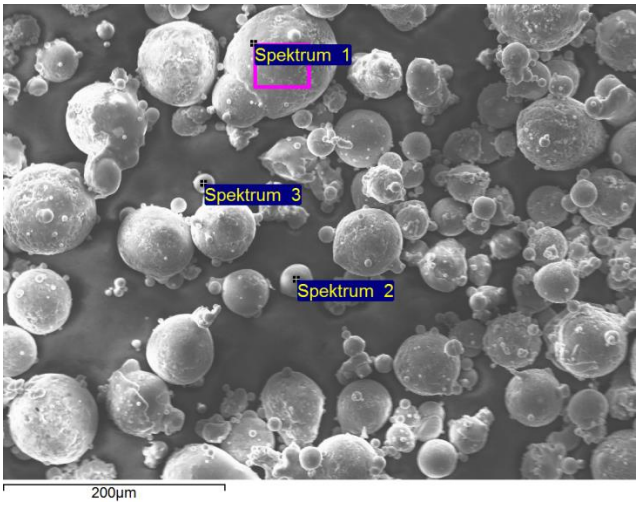

Element (mass %)	Al	Mn
Spectrum 1	86.1	13.9

Figure 3.2-3: Secondary electron image and selected EDX analysis of a sample of the coarse powder fraction before sieving.

3.3 Atmospheric plasma spraying of the AlMn12 alloy powder

3.3.1 Sample preparation

High strength 42CrMo4 steel plates were used as the substrate, and prepared for coating by first washing with soap to remove any oil or cutting fluid left over after machining. The dry plates were then sand blasted on one side with F36 alumina granules at a pressure of 4 bar to create a coarse coating surface. The plates were then cleaned with Langguth SC19 bio alcohol, and plasma coated with the alloy using a single pass sequence of an automated spray gun. A micrometer screw gauge was used to measure each sample before and after spraying to provide the thickness of each coating. Samples pieces were then cut from each plate, using a ATA Brilliant 250 cutting machine and then mounted in resin and polished down to 0,04 µm smoothness on a Struers TegraPol-31. The structure density, hardness and homogeneity were analysed using a Buehler micro hardness tester, Keyence VHX-2000 digital microscope and occasionally also a LEO 1450VP electron microscope with EDX capability. Samples used for corrosion tests were also glass peened at a pressure of 2 bar to increase the smoothness of the coated surface.

3.3.2 Process optimisation

Having successfully obtained the alloy feed powder the right set of operating conditions of the equipment needed to be determined. Atmospheric plasma spraying is well known for having a considerable number of adjustable operating parameters that needs to be individually adjusted to obtain the best results for a specific coating application. As a starting point the process parameters suggested in the Plasma-Technik AG operating manual for pure aluminium (< 45 µm) were used. By varying the current, standoff distance, argon volume, feed rate, injection angle and carrier gas pressure 18 combinations of thermal spraying parameters were tested to find the set that produced the densest and most homogeneous coating.

The biggest difficulties encountered with the plasma sprayed coating were the presence of unmolten and partially molten feed powder particles inside the layer, as well as internal and interface porosity which would negatively influence the adhesion and corrosion resistant properties of the coating. Of all the parameter combinations tested sample number 18 with the higher carrier gas pressure and 90° injection angle produced the best quality coating at a standoff distance of 14 cm. Throughout the entire length of the sample the alloy coating had a very homogenous and uniform structure.

The polished cross sections in Figure 3.3-1 illustrates the improvement of the coating quality when comparing the first and last samples, most notable is the improved density, better substrate contact and significant reduction in unmolten and partially molten powder in the layer. The outer surfaces were still very coarse as the samples had not been glass peened.

Table 3-2: Equipment parameters used for the first six samples.

Sample	Current (A)	Distance (cm)	Argon (l/min)	Feed rate (g/min)	Injection angle	Carrier gas (bar)	Measured Thickness (µm)
1	550	10	50	30	105°	1.5	140
2	550	12	50	30	105°	1.5	110
3	550	14	50	30	105°	1.5	110
4	550	10	60	30	105°	1.5	140
5	550	12	60	30	105°	1.5	120
6	550	14	60	30	105°	1.5	110
7	600	10	50	30	105°	1.5	120
8	600	12	50	30	105°	1.5	120
9	600	14	50	30	105°	1.5	120
10	600	10	60	30	105°	1.5	120
11	600	12	60	30	105°	1.5	130
12	600	14	60	30	105°	1.5	130
13	500	10	50	30	90°	1.5	120
14	500	12	50	30	90°	1.5	100
15	500	14	50	30	90°	1.5	100
16	500	10	50	30	90°	2	110
17	500	12	50	30	90°	2	90
18	500	14	50	30	90°	2	80

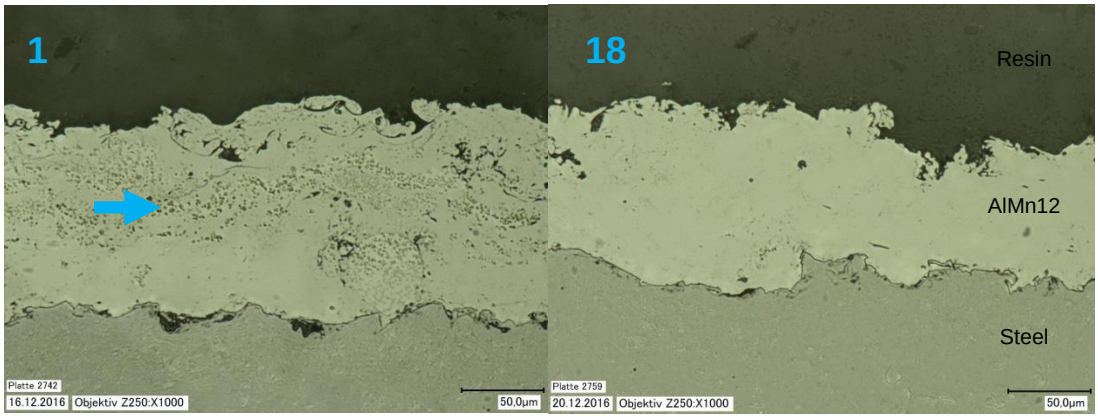

Figure 3.3-1: Micrographs at cross sections of the APS coatings on samples #1 and #18.

Metallographic analysis indicated that the quantity of un-molten feed powder retained inside the coatings did decrease to a large extent, but inevitably some partially and un-molten feed powder was still present. On the other hand the internal porosity was very low, giving the final layer a smooth and uniform appearance with thickness measurements before and after spraying indicating increased compactness.
It was felt that the processing setup used for sample #18 could not be improved upon any further and therefore these settings were subsequently used to coat some larger plates for bend, boil and neutral salt spray tests. The hardness of the coating remained in the same range as before with an average value of 130 ± 10 $Hv_{0.1}$.

EDX analyses of the coating surface again showed a slightly higher manganese content than the 12 mass % aimed for, possibly indicating that some aluminium was lost during the manufacturing and application processes (Figure 3.3-2). The alloy composition did however still remain within the ideal 12-14 mass % manganese range indicated by the electrochemical measurements above.

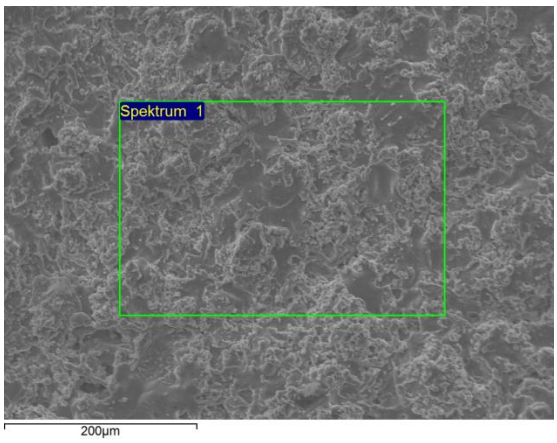

Elements (mass %)	O	Al	Mn	Sum
Spectrum 1	4.17	83.02	12.81	100

Figure 3.3-2: Backscatter electron image of the coating surface with EDX analyses on the right.

3.4 XRD analysis of the alloy powder and sprayed coatings

XRD analysis of the atomized alloy powder before spraying yielded an excellent fit with the diffraction pattern of aluminium, with a slight increase in the 2θ angle and some broadening of the peaks (Figure 3.4-1), and did not reveal the presence of any intermetallic compounds. Figure 3.4-2 shows the comparison in the diffraction pattern of the raw powder with that of the alloy that forms after atmospheric plasma spraying. The cooling rate experienced by the alloy particles are faster during plasma spaying than that experienced during atomizing, and as a result it could be seen that the 2θ angle of the peaks shift even more to the right. Also of interest to note is that the peaks measured after APS are again not only broader but form twin peaks, which with the diffraction pattern closely matching that of aluminum, indicating that rather than intermetallic compounds the alloy possibly consists predominantly of two types of super saturated aluminium, one with a higher and one with a lower manganese content.

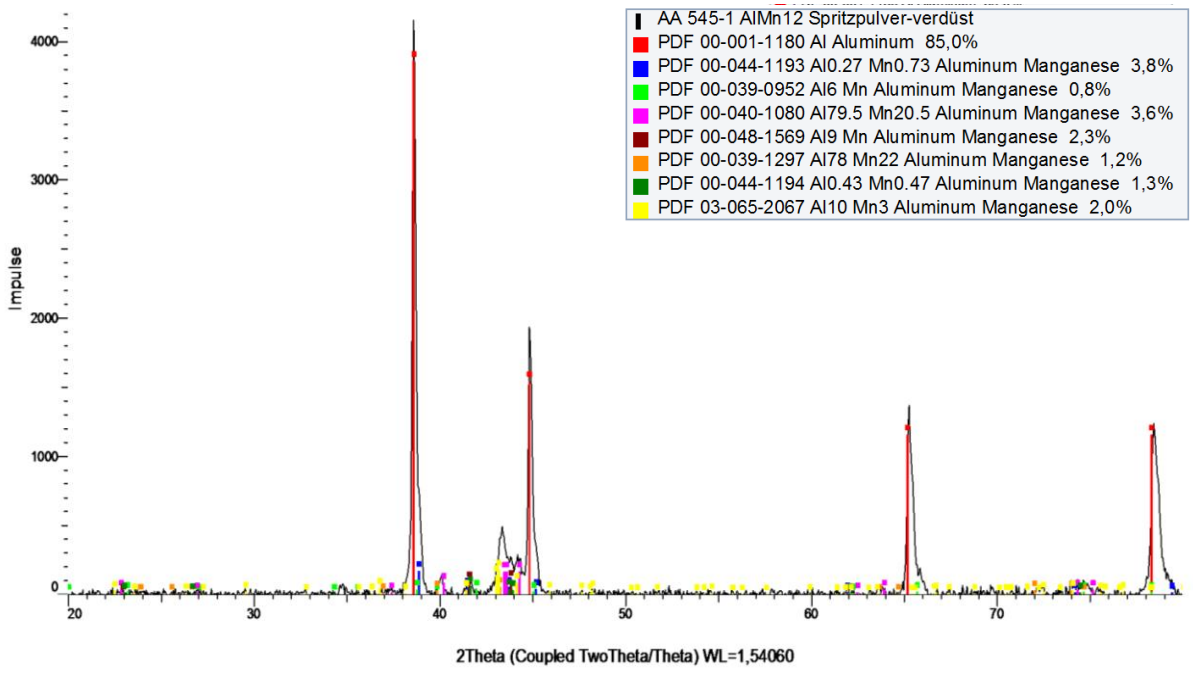

Figure 3.4-1: X-ray diffraction pattern of the atomized AlMn12 powder.

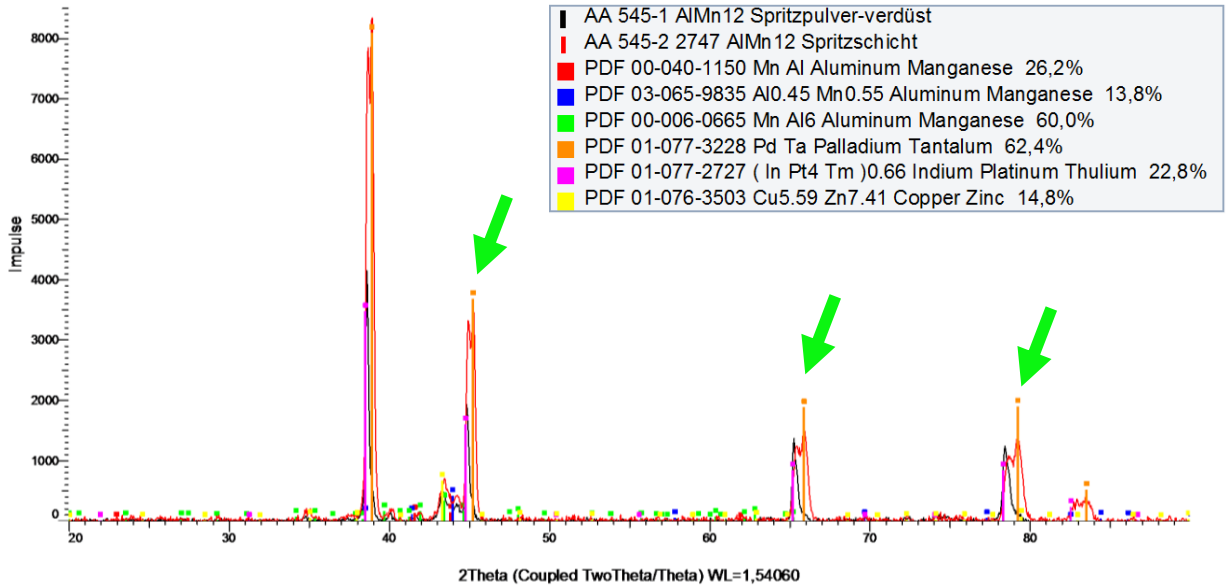

Figure 3.4-2: X-ray diffraction patterns of the AlMn12 powder before and after plasma spraying.

4 Corrosion resistance

Having succeeded in obtaining a suitable alloy and application method, the corrosion resistance of this combination needed to be evaluated. To obtain a relative indication of the alloy's performance it was evaluated against steel coated with pure APS aluminium, as well as industry supplied steel plates coated with ED cadmium, and ED cadmium with a chromate conversion coating.

XRD analyses had already indicated that the AlMn12 coating did not contain any measureable quantity of intermetallic phases, therefore anodic polarization measurements were done once more to reveal whether this phase change improved the electrochemical properties of the alloy as was expected, and then compare it against the results obtained from the commercial samples. This was followed by laboratory scale salt bath submersion tests using samples with and without surface passivation, as it is a fast method for obtaining indicative results on the performance of the coatings in a severely corrosive environment. The AlMn12 alloy was then subjected to a standardized ISO 9227 / ASTM B117 neutral salt spray test, while bend and boil tests were also used to obtain an indication of the level of adhesion between the alloy and the steel substrate. It should be noted beforehand however that as stated in the standard guide for laboratory immersion corrosion testing of metals (ASTM G31), that '…*experience has shown accelerated corrosion tests only give indicative results, and may even be entirely misleading'*.

Ultimately many more standardized and accredited chemical, mechanical and corrosion tests will need to be done to show the true level of conformance with aviation build and safety specifications, which falls outside the limitations of this investigation. Nevertheless, these test results still serve to substantiate the purpose of this project in providing a proof of concept regarding possible future solutions for the aerospace industry to comply with new environmental regulations.

4.1 Anodic polarization measurements.

During the screening tests conducted on furnace cooled bulk alloy samples the AlMn12 alloy showed some promise as its corrosion potential was more positive than that of aluminum, but with the disadvantage of having a higher corrosion current density. It was expected that the electrochemical characteristics of the alloy would improve after plasma spraying, but to which degree was uncertain. Repeating the anodic polarization of the AlMn12 alloy, this time after plasma spraying, the significant influence of the cooling rate on its corrosion resistance was clear. The polarization potential became slightly more negative, however the corrosion current density showed considerable change and decreased by two orders of magnitude, most likely brought about through minimizing the formation of unwanted noble intermetallic phases by retaining the manganese in solid solution (Figure 4.1-1).

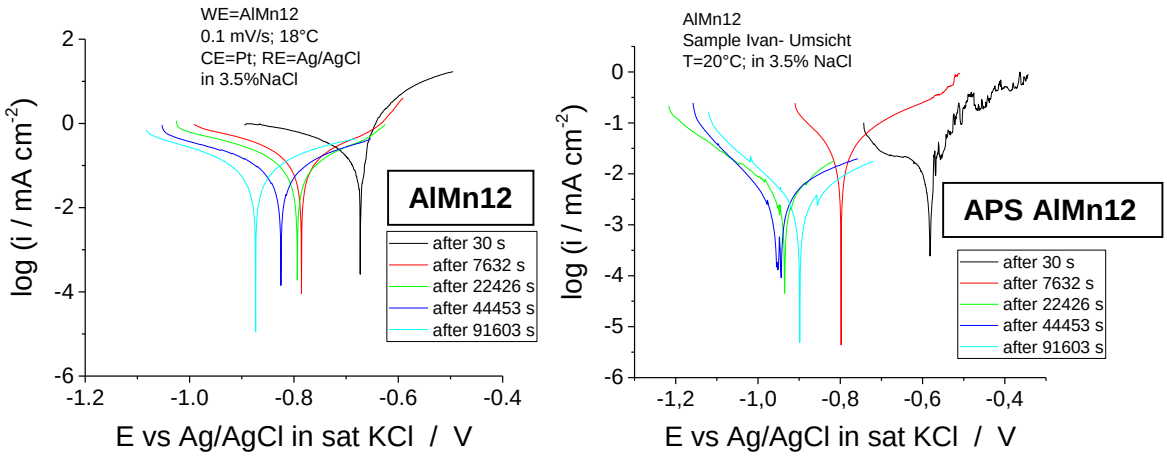

Figure 4.1-1: Effect of cooling rate on the polarization behaviour of the AlMn12 alloy, with furnace cooling on the left side and atmospheric plasma spraying on the right.

Table 4-1: Influence of cooling rate on the polarization characteristics of the AlMn12 alloy.

Al-Mn12 Alloy	Furnace cooled	Plasma sprayed
E_{corr}(V)	-0,873	-0,899
I_{corr} (µA/cm²)	229,98	4,22

The corrosion resistance of the control sample of pure atmospheric plasma sprayed aluminium, and the two industry supplied samples of ED cadmium and ED cadmium with a chromate conversion coating (which is currently the industry gold standard), were also potentiodynamically evaluated with the results indicated in figure 4.1-2 below. The comparative results, shown in table 4-2, indicate that the AlMn12 coating should be competitive, with a corrosion current density similar to that of aluminium but significantly lower than that of cadmium. As expected the corrosion potential of the alloy improved and is more positive than that measured for pure aluminium, but still less than the corrosion potential of the cadmium coatings.

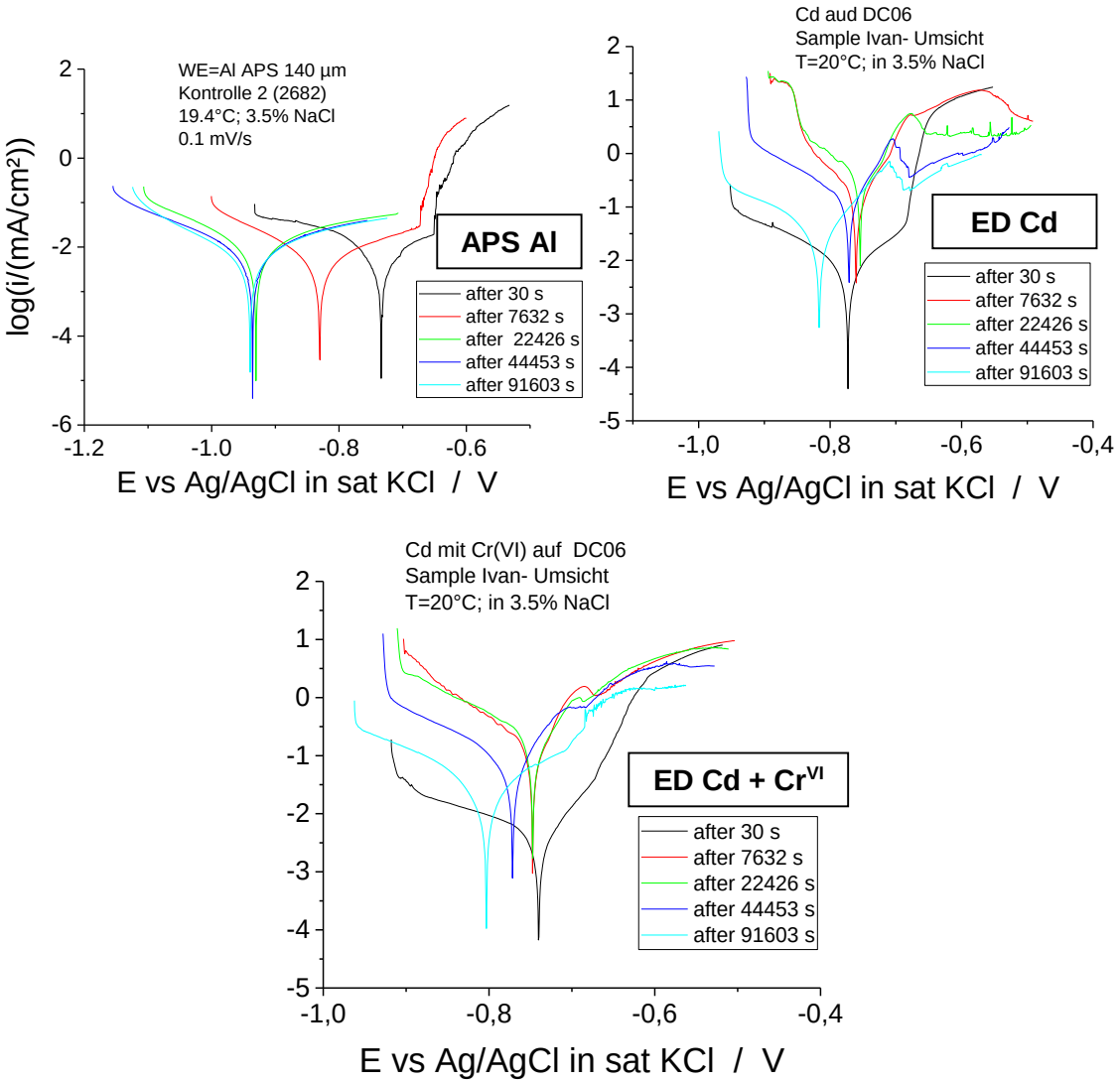

Figure 4.1-2: Anodic polarization measurements of APS Aluminium (top left), electroplated Cd (top right) and chromated Cd (bottom).

Table 4-2: Summary of the polarisation characteristics measured for the test samples.

	Aluminium	Al-Mn12 Alloy	Cadmium	Chromated Cadmium
E_{corr}(V)	-0,940	-0,899	-0,803	-0,816
I_{corr} (µA/cm²)	7,04	4,22	45,07	43,24

Theoretically therefore this alloy compares favorably with its industrial competitors, with the coating evidently having the potential of providing sacrificial protection to a high strength steel substrate while maintaining a low rate of corrosion.

4.2 Salt bath experimental procedure

The experimental setup consisted of a 1000 ml glass beaker filled with 500 ml of deionized water, with a NaCl concentration of 5 mass %. A hot plate and magnetic stirrer were used to keep the solution agitated and at a constant temperature of 35°C, while a rubber tube connected to a peristaltic pump kept the solution aerated.

Samples were suspended into the solution using a piece of aluminium wire, covered with isolation tape, to prevent any direct metal to metal contact. In addition a watch glass and paraffin tape was used to seal off the beaker to prevent evaporation of the solution during testing. The sample plates used were 3 x 3 cm high carbon CrMo steel (AISI 4140) with a thickness of 3 mm, with a 4mm hole drilled through the top side of each plate to allow them to be suspended in the solution. Before being submerged the samples were weighed and isolation tape attached onto the back and sides to seal off the remaining steel surfaces. Once a day the samples were removed and furnace dried at 105°C for 15 minutes and then weighed and photographed before being returned to the solution.

4.3 Salt bath corrosion of AlMn12

As mentioned above pure APS aluminium coating have been qualified for use on some of the larger landing gear components of military aircraft. To see if the AlMn12 alloy provided any significant improvement two plates coated with a 100 µm thick layer of the AlMn12 alloy were placed in the aerated salt bath alongside two similar plates coated with 100 µm of pure aluminium. One plate from each set was scribed deep enough to expose the underlying steel substrate.

In the images displayed below it can be seen that at the conclusion of the submersion test the amount of corrosive residue that formed on the surface of the AlMn12 coated alloy was slightly less than that on the aluminium coated samples. Weight loss measurements of the cleaned plates confirmed this with the AlMn12 coating having lost 0,010% of its mass, compared to 0,026% for the aluminium coating (Figures 4.3-1 & 4.3-2).

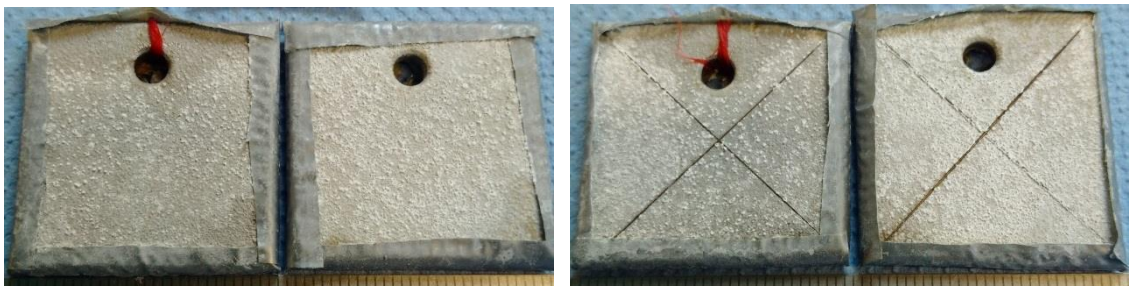

Figure 4.3-1: AlMn12 (left) and pure Al (right) plasma sprayed plates after 48 hours in the salt solution.

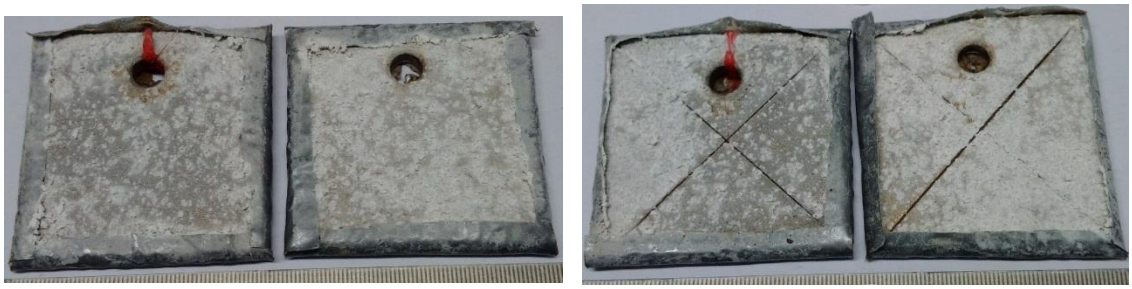

Figure 4.3-2: AlMn12 (left) and pure Al (right) plasma sprayed plates after 120 hours in the salt solution.

On the negative side the AlMn12 alloy showed poor adhesion along some of the sample edges after thermal spraying, with the condition of these areas deteriorating even more during the corrosion test as shown in figure 4.3-3. Similar adhesion problems were not present on the flat surface, even after the coating had been scratched. It is therefore unclear whether the poor attachment on some of the edges was due to the angled geometry, poor surface preparation (sand blasting) or the coating procedure. Even if the corrosion resistance of the alloy proved to be significantly better than pure aluminium during long term corrosion testing, poor adhesion to irregular surfaces such as sharp edges and corners can render it unsuitable for coating any complex components.

Figure 4.3-3: Illustration of flaking edges of AlMn12 coated sample after 120 hours in the salt solution.

4.4 Salt bath corrosion of aluminium and cadmium based coatings.

The test was repeated using the same experimental setup, but with an increased volume of solution to allow for the simultaneous submersion of eight samples. Four of the samples were again high strength AISI 4140 grade steel, two of which were plasma sprayed with aluminium and two with the AlMn12 alloy. In addition to the APS coatings all four plates were also conversion coated with the experimental Mn-V hexavalent chromate alternative as described later on in Part B.

The remaining four samples were industry supplied control samples consisting of DC06 steel plate covered with electrodeposited cadmium. Two of these samples were also chromate conversion coated (Cr^{VI}) which account for the golden color (Figures 4.4-1 & 4.4-2). As before one sample from each set was scribed and the other left undamaged. Tape was used to seal off the back and sides of all eight plates, leaving only one surface exposed to the solution. The position of the plates were also rotated on a daily basis after photographs and weight measurements were taken to minimize any possible influence their position in the bath relative to the air hose or magnetic stirrer might have.

Figure 4.4-1: Mn-V conversion coated samples at 0 hours; AlMn12 on the left and pure Al on the right.

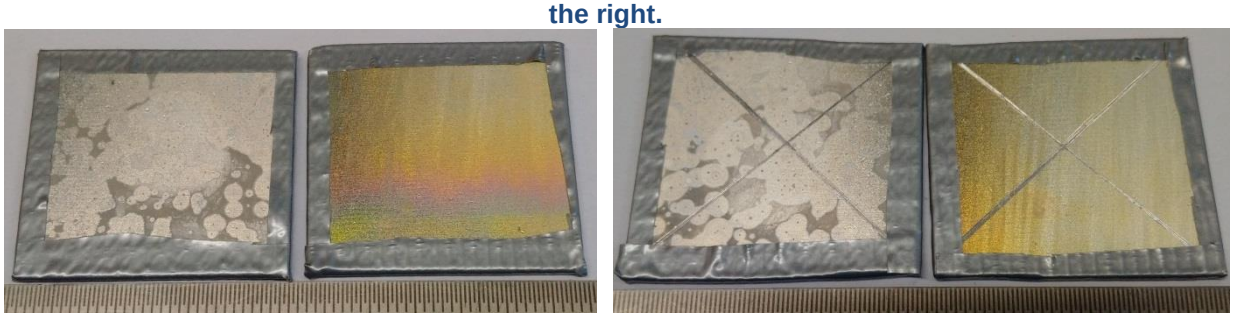

Figure 4.4-2: Industrial control samples at 0 hours; silver electroplated Cd on the left and Cd with golden chromate conversion coating on the right in both photos.

Figure 4.4-3 shows the visual results after 96 hours of submersion in the aerated salt bath. The most obvious and noticeable difference being the large volume of corrosion product that was generated on the aluminium based coatings. The low volume of corrosive products generated by cadmium is one of its well-known properties that has made it such a desirable coating of fasteners in the aviation industry as it does not seize up tight, low tolerance or threaded components. It should be kept in mind however that complete submersion in a corrosive environment initiates a very high rate of corrosion, and that aluminium coated plates corroded at a slower rate in a neutral salt fog chamber does not generate such high quantity of corrosive product on the surface as seen here. It's suitability for use on tight tolerance components should therefore be investigated separately.

Figure 4.4-3: Sample plates after 96 hours in the salt bath, from left to right Al, AlMn12, Cd and Cd + Cr^{VI}.

The cadmium based samples had virtually no corrosive product formation on top of the surface, yet weighing of the cleaned samples showed that the appearance was somewhat misleading, as all four aluminium based coatings outperformed their cadmium rivals by an order of magnitude as shown below in table 4-3.

Table 4-3: Percentage weight lost by each type of coating after 96 hours of corrosion.

% Weight lost							
Al + MnV		**AlMn12 + MnV**		**Cd**		**Cd + Cr^{VI}**	
Plain	Scribed	Plain	Scribed	Plain	Scribed	Plain	Scribed
0,041%	0,075%	0,089%	0,049%	0,176%	0,186%	0,124%	0,159%

There was little to distinguish between the performance of pure aluminium compared to the aluminium-manganese alloy, with one performing better in the plain condition and the other better when scribed. The formation of such a large quantity of aluminium oxide on the surface of these samples might have had a passivating effect by sealing off large areas of the exposed surface from contact with the solution, and also explains why the scribed AlMn12 plate performed better than the undamaged plate. With the corrosion residue removed the coating surfaces that were exposed still appeared in good condition (Figure 4.4-4), except for the edges where any slight detachment of the isolation tape would have resulted in crevice corrosion, and should therefore not be considered.

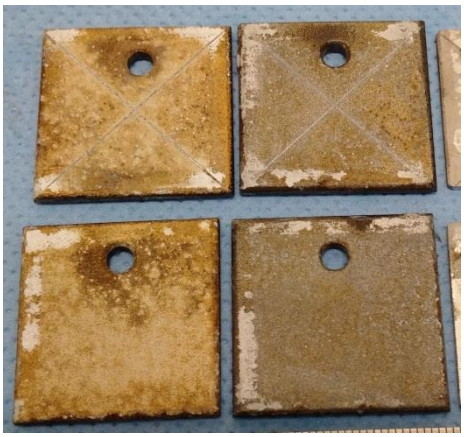

Figure 4.4-4: Surface condition of Al and AlMn12 sample plates after 96 hour with the tape and corrosion residue removed.

Another factor that could have had a small influence, particularly on the scribed plates is that the industry supplied samples are coated onto low carbon steel which would have a slightly different corrosion potential than that of the high carbon steel. Nevertheless the corrosion weight loss results mimic the prediction of the anodic polarization measurements i.e., that the aluminium based coatings will corrode away at a slower rate than the industrial cadmium coatings.

4.5 Bend and boil adhesive tests

To investigate the level of adhesion achieved between the AlMn12 alloy and high strength steel a sample plate was placed into boiling water for three hours together with an aluminium coated plate. Neither plate showed any signs of damage or detachment. This was followed by bend adhesion testing of coated 2 x 10 cm plates, first to a 90° angle and then to a 180°angle (Figures 4.5-1 & 4.5-2).

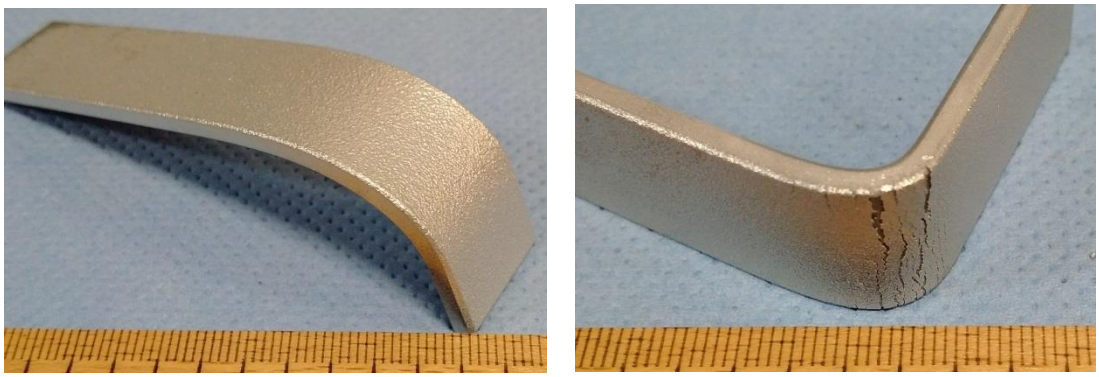

Figure 4.5-1: Results of the 90° bend test of plasma sprayed aluminium (left) and aluminium-manganese alloy (right).

Figure 4.5-2: Results of the 180° bend test, three AlMn12 samples on the left and one conversion coated Al sample on the right.

The results of the bend test shown in figure 4.5-2 clearly indicate the poor adhesion between the AlMn12 alloy and high carbon steel. For all plates shown above the exact same substrate, surface and corner preparations were used. The pure conversion coated aluminium layer had much better adhesion, with no damage visible after the 90° bend, and only a few tiny cracks on the edges after the 180° bend. According to military test specifications "*cracking is acceptable in the bend area if the coating can not be peeled back with a sharp instrument*" but separation such as flaking or peeling is not acceptable (JTP BD-P-1-1)[23]. However how crucial the outcome of the bend adhesion test is, might be debatable as to the relevance of

corrosion resistance of high strength steel components after having being physically destroyed and no longer suitable for service. The plasma sprayed AlMn12 alloy was not brittle with an average hardness of 130 $Hv_{0.1}$ and could be boiled, dropped, scratched and shot peened without showing any signs of damage or detachment.

4.6 Neutral salt spray testing

Shown below in figure 4.6-1 for example is the corrosion results of an Al60Mn40 APS coating previously created by A. Förg and tested by the CRM Group. After the first day of exposure the areas of weakness or high activity starts to become visible due to discoloration and streaking of corrosion residue. As the test progresses the affected areas only continue to degrade further. Rust formation is not instantaneous as it takes time for the substrate to be reached, 240 hours in this case, but the impending failure is clearly exposed early on.

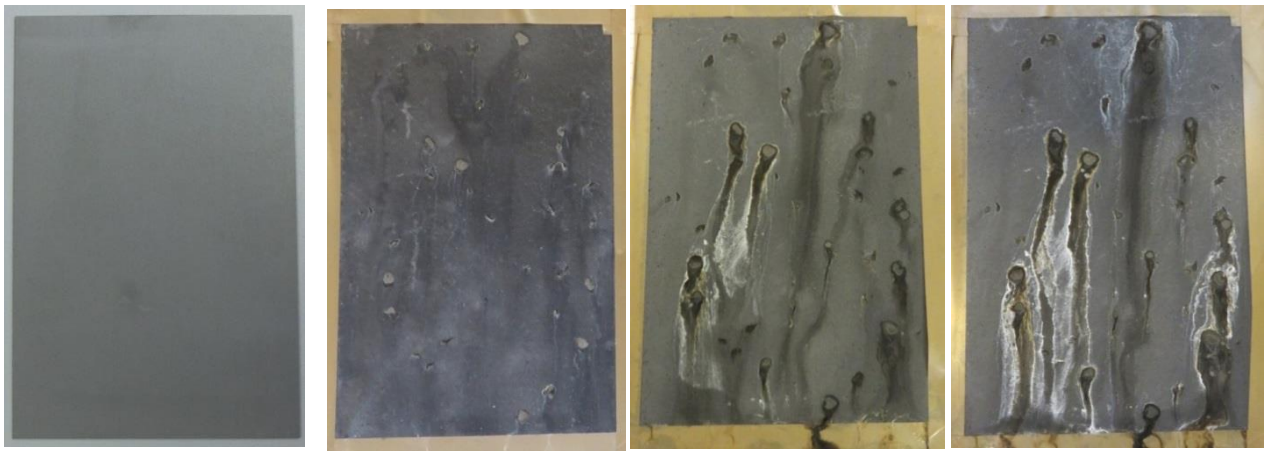

Figure 4.6-1: Al60Mn40 alloy on 42CrMo4 steel after 0, 24, 144 and 240 hours salt fog exposure (A. Förg & the CRM Group).

For the AlMn12 alloy two 10 x 15 cm 42CrMo4 steel plates were tested according to ISO 9227 / ASTM B117 neutral salt spray specifications at the Technical University of Ilmenau for a duration of 300 hours. Before the test the back and sides of the plates were sealed off with a waterproof lacquer. The coating performed well in both conditions with the slight streaking visible clearly originating from the edges and holes which fall into the 1 cm exclusion zone. The lack of corrosion hot spots, pitting or rust formation indicates that the alloy has some potential as a corrosion resistant coating as it displayed high levels of both barrier and sacrificial protection (Figures 4.6-2 & 4.6-3).

Figure 4.6-2: Plasma sprayed AlMn12 alloy on 42CrMo4 steel substrate after 0, 26 and 300 hours of salt spray corrosion.

Figure 4.6-3: Scribed sample of plasma sprayed AlMn12 alloy on 42CrMo4 steel substrate after 0, 26 and 300 hours of salt spray corrosion.

Also note in contrast to the samples that were submerged in a salt water solution, the complete lack of corrosive residue build up on the surface. This demonstrates the influence of the corrosion rate on the mechanisms being experienced by the coatings. Unfortunately the actual natural corrosion rate to which the coatings are subjected during service is too slow to use as a testing method, thereby necessitating the use of artificially accelerated tests, which may not be a realistic representation but still provides a sufficient indication of acceptable performance. Postmortem analysis of the samples were not possible, however the black discoloration around the scribe and edges would most likely be Mn^{IV} in the natural oxide form as MnO_2 that remains after the aluminium oxide rinsed away as the lighter colored streaks.

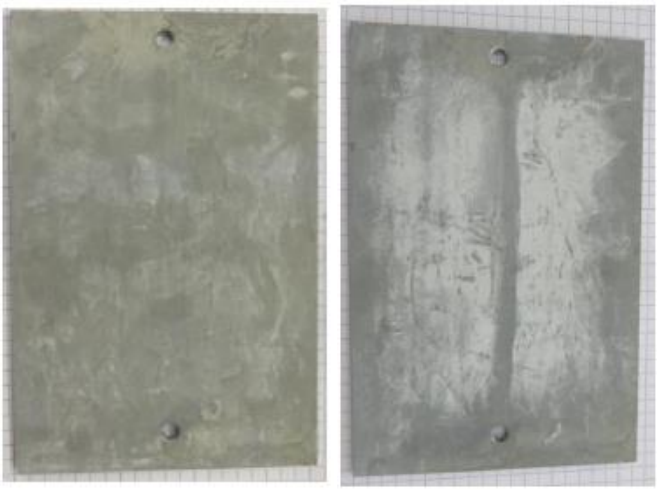

Figure 4.6-4: Cadmium plated 42CrMo4 steel after 240 and 1000 hours of neutral salt spray testing courtesy of the CRM Group.

For comparison figure 4.6-4 shows the results of the same 42CrMo4 steel electroplated with cadmium, after 240 and 1000 hours of neutral salt spray exposure as tested by the CRM Group. The indisputable quality of a cadmium coating is clearly demonstrated with the lack of streaking, pitting or discoloration even after 1000 hours. These initial test results of the atmospheric plasma sprayed AlMn12 alloy on high strength steel was positive, and long term corrosion tests can now be done to reveal the full potential of this alloy, and to determine whether or not it can become a possible alternative for the use of cadmium.

5 Conclusion on AlMn as a cadmium substitute

When looking at the obtained results the AlMn alloy does appear to have some potential for the protection of high strength steel components. However even though the alloy is environmentally friendly and possesses good electrochemical characteristics, it also has its own challenging properties such as adhesion that needs to be managed.

Using atmospheric plasma spraying as the application method was cost effective, did not require hydrogen baking and had low enough deposition temperatures to allow its use on ultra-high strength steels, but the method also has its own inherent limitations such as application thickness, rough outer surfaces and inability to coat internal surfaces which do not always meet the specified requirements.

At the end of the day after having conducted the various tests as described above, it is not yet clear whether or not a plasma sprayed aluminium-manganese alloy provides any significant advantage over pure aluminium in terms of corrosion resistance. Pure aluminium is very susceptible to pit formation in a chloride environment, which is its typical mode of failure during NNS testing. If the AlMn alloy is more resistant to pitting corrosion it might still be suitable for some selective large landing gear components baring its failure of bend adhesion. Under normal conditions however the coating adhesion is stable and can be scratched, dropped, boiled and shot peened without detaching. Its adhesion only fails during serious damage and deformation of the substrate, but being an alloy its composition still has the ability for some adjustment; a decrease in manganese content should improve the ductility and adhesion properties to some degree.

Theoretically therefore the corrosion potential and lower reactivity of the plasma sprayed aluminium-manganese alloy could potentially make it a suitable replacement for cadmium on selective high tolerance components, yet further testing and refinement is still required.

6 Part B: Development of a permanganate-vanadate conversion coating (PVCC) as a Cr^{VI} replacement

Aviation build and test specifications require cadmium coated surfaces to receive an additional chromate conversion surface passivation before use. As described above, this thin ion rich chromate layer has a significant beneficial influence on the corrosion resistance in a salt water environment as its entrapped Cr^{VI} ions firstly repel negatively charged chlorine ions, and secondly has the ability to heal itself through the diffusion and formation of new Cr^{III} oxyhydroxide at damaged sites. The application process is very simple and efficient, only requiring submersion of clean and activated parts into a chemical coating bath for 3-5 minutes. Unfortunately this simple and highly effective treatment is centered around the behavior of the carcinogenic Cr^{VI} ion.

The chromate conversion coating process remains in use as a suitable alternative has not yet found widespread acceptance, but the implementation of REACh regulations has now forced the aviation industry to find and qualify a more environmentally friendly solution to replace the current chromate process. However since the production schedules of the extensive and complex global network of component manufacturers continuously supplying the aircraft assembly lines should preferably not be disrupted, it is imperative that any new conversion coating process maintains similar processing steps and treatment times to allow a seamless change over. In order to comply with REACh regulations and provide the industry with a more environmentally friendly corrosion resistant solution, which can potentially remove both cadmium and its accompanying Cr^{VI} surface passivation, a new experimental conversion coating was also developed and tested.

The application of a conversion coating typically consist of a multi-step process where the components are submerged in a treatment solution followed by submersion into two rinsing baths before the next treatment step. Figure 6-1 illustrates a typical conversion treatment sequence for aluminium components.

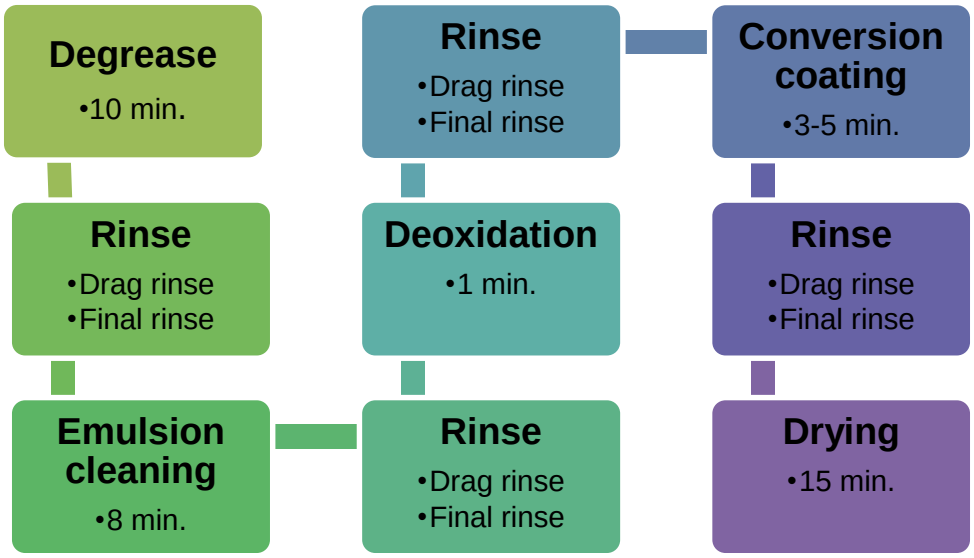

Figure 4.6-1: Typical conversion coating sequence used for aluminium components.

The overall process takes roughly 30-45 minutes depending on whether the components are dried or not. It is therefore critical that any new conversion coating reactions are completed within a 3-5 minute timeframe. Many proposed alternatives have fallen short of this requirement by for example requiring 20 minutes of reaction time, which increases the total production time to around 50-60 minutes and subsequently nearly halves the production rate of the processing line, which from an economic standpoint is unacceptable. In order therefore to produce a viable alternative coating, the same treatment steps and times should preferably be adhered to, to avoid any additional infrastructure or reduced production output.

The aim of the new conversion coating was to produce a primary manganese oxide based surface structure with some retained or entrapped higher valence metal ions (Mn^{VII}, Mo^{VI}, V^{V}) to provide active corrosion protection similar to Cr^{VI}. Initial experimentation was done using potassium permanganate, sodium nitrate and lithium fluoride, and once satisfactory coating process parameters were established molybdate and vanadate were also added. The vanadate displayed a high degree of self-healing and readily passivated any open steel surfaces, while the molybdate on the other hand did not react at all and was subsequently left out of the coating solution. The resulting permanganate-vanadate coating displayed good adhesion on pure aluminium surfaces and performed well in the ISO 9227 neutral salt spray test with the final coating having many of the properties desired by industry. The use of standard processing steps and reaction times combined with a coating bath chemical composition not affected by European REACh regulations, could potentially allow this chromium free conversion coating to become a future alternative drop in replacement for Cr^{VI} based surface treatments.

Laboratory scale salt bath submersion, adhesion tape testing and neutral salt spray tests were used to obtain an indication of the performance of this new coating when applied to high strength steel samples coated with a layer of APS aluminium. Neutral

salt spray testing (ISO 9227/ASTM B117) is commonly used for evaluating the corrosion resistance of unpainted conversion coatings. The results of this test method has however been called onto question, as the accelerated rate of corrosion may in fact alter the corrosion mechanism itself[45]. The pass/fail criteria is established by industrial specifications, but are usually assessed through the time lasted until the appearance of red rust or the allowable limit of corrosion pits per specified area within a specified amount of time is reached, e.g. five or more pits on a 10 x 15 cm sample within 168 hours constitutes a failure. The area within 1 cm from the sample edges is generally left out of consideration due to the influence of the exposed substrate.

The evaluation of this criterion is possibly the most controversial aspect of this test method, as it relies almost entirely on the examiners judgement and experience in deciding when to count a pit, which can be active/weeping, closed off by corrosion product, big or small, clustered together or isolated etc. Nevertheless despite its controversy the salt fog test remains popular and is commonly used in many industries as a benchmark, the results of which might not be able to distinguish good from very good, but can separate poor from excellent[45].

The industrial control used to provide a reference point for the test results was the Cr^{III}-Zr coating, which is currently one of the most likely alternatives being vetted for use in the aviation industry. It provides a decent level of corrosion resistance but its shortcomings are a lack of color that hinders quality control, no self-healing ability and the concern that Cr^{III} can oxidize to Cr^{VI} during corrosion.

In summary, there are a wide variety of alternatives that have been proposed as replacements for the CCC process. All of these alternative processes first need to be subjected to a considerable amount of comparative testing and evaluation to determine the most suitable and economic solution, before a replacement process can be certified and adapted for worldwide industrial use. There are many factors such as cost, adhesion, colour or processing time for example that can render a coating unsuitable for aerospace application. While even if a suitable green process is approved it still remains very difficult to implement large scale changes in the build specifications of any aircraft, as the manufacturing life span of all models are very long and involves manufacturing contracts with a large number of global suppliers. The service life of each aircraft also span several decades, throughout which components corresponding to the original build specifications must be repairable during maintenance and service. Nevertheless the implementation of strict environmental regulations like REACh, RoHS and ELV will eventually lead to the complete removal of cadmium and hexavalent chromium from the production cycle.

6.1 Experimental procedure

The substrate material used was 42CrMo4 (AISI 4140) high strength steel plate, with a thickness of 4mm. The steel was coated with a 140µm thick layer of aluminium (Oerlikon Metco 54NS 99% pure) applied using atmospheric plasma spraying and glass peened for smoothness. The industrial control samples used the same substrate but was coated by SurTec Deutschland GmbH in Zwingenberg with a Cr^{III}-Zr based conversion coating known commercially as *SurTec650 chromitAl* (US patents 6375726; 6511532; 6521029; 6527841).

The experimental processing sequence illustrated in figure 6.1-1, started with a degreasing wash with soap and tap water rinsing, that was followed by 5 minutes of ultra-sonic cleaning in a Bandelin Sonorex RK52 using Langguth SC19 bio alcohol followed by drying with hot air. The aluminium oxide surface layer on the samples was then removed using an alkaline etching pre-treatment in a 2 mass % NaOH solution at 50°C followed by two stage rinsing in de-ionized water.

The plates were then immediately suspended inside the agitated coating bath with a solution temperature of 75°C for 3-30 minutes. The coating bath pH was monitored with a Griesinger GPHR 1400 digital pH/mV meter and sodium hydroxide crystals and diluted nitric acid used for adjustments to ensure that the bath pH remained close to 11. After treatment the samples were again subjected to a drag rinse and final rinse in de-ionized water, and then left to dry and cure for 48 hours, after which optical analysis of the coatings were done using a Keyence VHX-2000 digital microscope and occasionally also a LEO 1450VP electron microscope with EDX capability.

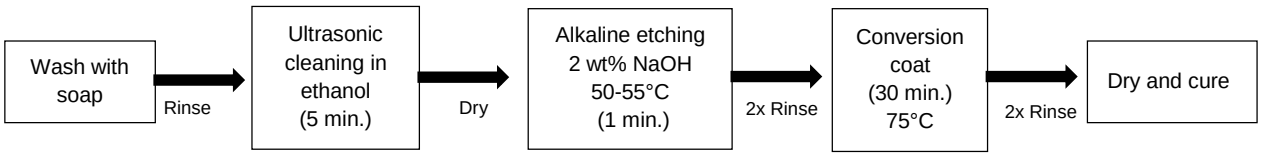

Figure 6.1-1: Processing sequence used for the experimental conversion coating.

6.2 Experimental setup

Laboratory salt bath submersion testing was done using a glass beaker containing 500 ml solution of de-ionized water with a salt concentration of 5 mass % NaCl. The solution was continuously agitated using a magnetic stirrer, and aerated through a rubber tube connected to a peristaltic pump. During testing the top of the beaker was also sealed off using a watch glass and paraffin film to minimize evaporation of the solution. After every seven days the solution was discarded and replaced with a fresh batch. All ISO 9227 / ASTM B117 neutral salt spray testing and anodic polarization measurements and were done at the Technical University of Ilmenau, using a standard three electrode setup on a 0,13 cm^2 sample area in a 3,5 mass %

NaCl solution, with a platinum counter electrode, a Ag/AgCl reference electrode in a saturated KCl solution and a scan rate of 0,1 mV/s.

6.3 Experimental Development

Initially only $KMnO_4$ based solutions were used to establish and refine the coating process parameters, along with the addition of $NaNO_3$ and LiF which aided significantly in coating formation and adhesion. The permanganate based solution reacted readily to form golden colored surface coatings with the typical mud-cracked surface structure as shown in figure 6.3-1. Reaction times were also short allowing entire sample surfaces to be fully coated within 5 minutes, with the best quality coatings obtained at a pH of 11 without using any acid activation pre-treatment.

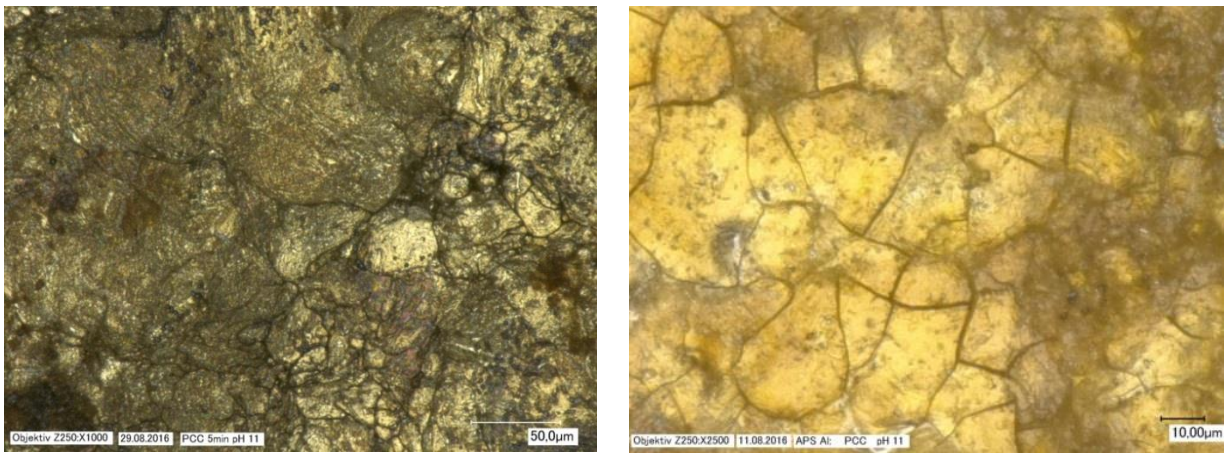

Figure 6.3-1: Two examples of the golden mud-cracked permanganate surface coatings obtained on plate samples. (Magnifications of approximately 1000x on the left and 2500x on the right)

Following this sodium-vanadate was also added into the solution to a concentration of 10 g/l; unfortunately this had a negative influence on the reaction time and coating formation of the permanganate. Little reaction took place at lower pH levels or short contact times. Processing for 30 minutes at a pH of 11, however, did eventually result in the entire surface being coated (figure 6.3-2). Take note that as stated previously the irregular surface condition is not part of the coating but rather the result of etching the uneven multilayered APS aluminium substrate, which reveal the boundaries of individual splat particles.

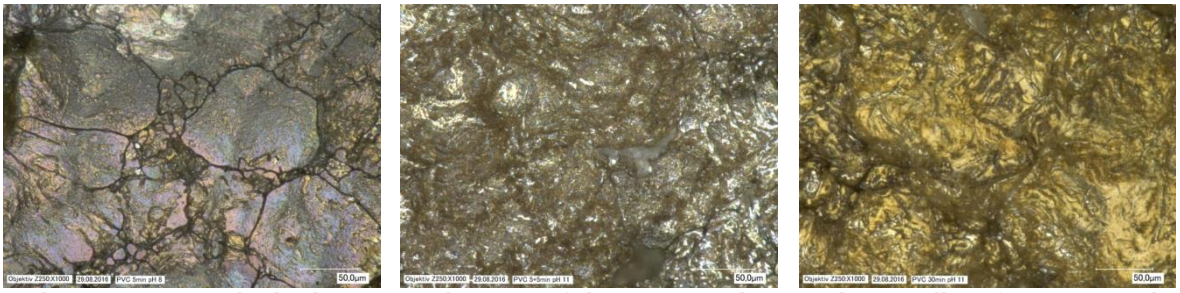

Figure 6.3-2: Optical microscope images of the progressive coating quality after 5, 10 and 30 minute reaction times following the $NaVO_3$ addition at approximately 1000x magnification.

Optical analysis revealed that after 30 minutes the entire surface was covered in a golden mud-cracked type coating, while a tape test showed that the coating also had good adhesion to the substrate, but that some of the darker colored residue on the surface were only superficial and not part of the coating itself (Figure 6.3-3).

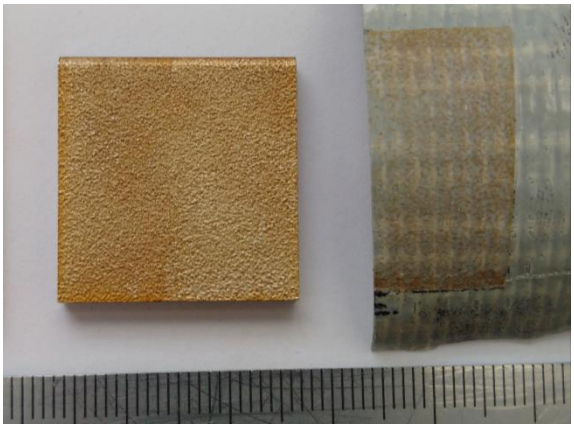

Figure 6.3-3: Adhesion tape test of dry coating of sample B.

When comparing sample B against the commercial control coating, the layer formed by the 1:1 Mn:V solution appeared very coarse with larger openings in the surface (figure 6.3-4). In light of the good layer forming ability observed when coating with manganese only, another sample was coated using an increased $KMnO_4$ concentration of 20 g/l to try and improve the heavily mud-cracked surface structure. This resulted in a coating with a slightly darker gold-brown appearance which did indeed have a more compact exterior and narrower cracks than before as indicated in figure 6.3-4 below.

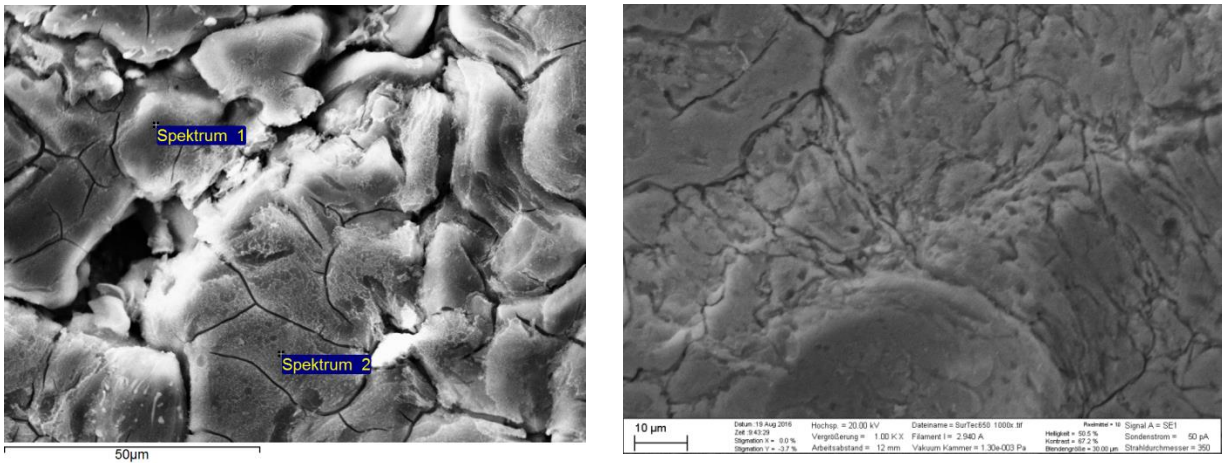

Figure 6.3-4: Backscatter electron images at equal magnification of PVCC coated sample B and the Cr^{III}-Zr coated control sample.

To select a final solution both samples treated in the 1:1 and 2:1 ($KMnO_4$:$NaVO_3$) solutions were placed in the aerated salt bath (5 mass % NaCl) at room temperature with the steel surfaces at the sides and back not covered up. After 4 hours the first signs of a white corrosion product appeared on the surface of sample B, and after

4.5 hours also just started to become visible on the surface of sample C, but to a lesser extent (Figure 6.3-5).

Figure 6.3-5: Mn-V 1:1 ratio (top) and Mn-V 2:1 ratio (bottom) after 0, 24 and 120 hours in the salt bath solution.

After 24 hours it became difficult to clearly and definitively distinguish between the performances of the two coatings, as white corrosion products had appeared on the surfaces of both. Based on the fact that the initial onset of corrosion was slower for the sample coated using the 2:1 ($KMnO_4$:$NaVO_3$) ratio, it was selected as the final coating solution to use for further testing. Coating at a higher pH was also attempted but aborted after it became evident that the coating solution buffered at a pH of 11. Table 6-1 gives a summary of the processing parameters and chemical concentrations of the coating bath solutions used to prepare some test samples. The hot alkaline etching times had to be increased for larger samples in order to achieve complete de-oxidation of the surface.

Table 6-1: Coating parameters of various test samples.

Sample	Substrate	pH	Time (min)	Hot alkaline etch (sec.)	$KMnO_4$ (g/l)	$NaVO_3$ (g/l)	$NaNO_3$ (g/l)	LiF (g/l)
A	Al on 42CrMo4	11	5	20	10	0	4	0.8
B	Al on 42CrMo4	11	30	45	10	10	4	0.8
C	Al on 42CrMo4	11	30	45	20	10	4	0.8

6.4 Corrosion results of the un-scribed plates

Four plates with dimensions of 30 x 30 x 3 mm with a 4 mm hole in one corner were suspended in the salt water solution for 336 hours. The aluminium surface of two of these plates contained the golden-brown PVCC passivation coating, while the two control samples contained the colorless Cr^{III}-Zr based commercial coating. To evaluate both the barrier and sacrificial corrosion resistance a corner to corner cross was also scribed on one plate of each set to expose the underlying steel substrate to the salt water. The option of taping up the plates was dismissed as there was no certainty of whether it would remain equally attached to all samples throughout the 14 day duration of the test, and could therefore possibly introduce some unwanted variance into the observations.

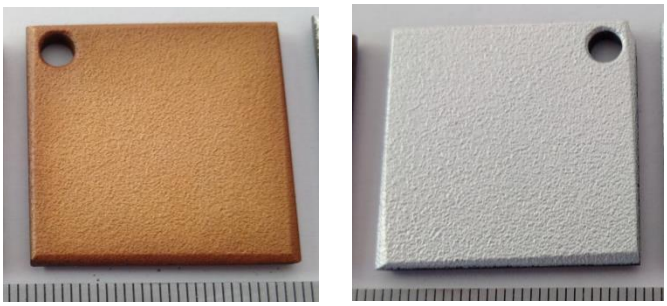

Figure 6.4-1: Sample plates before the corrosion trial, PVCC plates on the left and *SurTec650 chromitAl* on the right.

Figure 6.4-2: Sample plates after 24 hours (left) and 120 hour (right) of submersion.

Figure 6.4-3: Sample plates after 264 hours (left) and 336 hours (right) of submersion.

Figures 6.4-1 to 6.4-3 above indicates that the test samples experienced a very rapid rate of corrosion, with the first white corrosion product already visible to varying degrees on the surfaces of both samples within 24 hours. An additional series of photographs with slightly higher magnification are also included in Appendix 1 as the

initial quantity of corrosive product is not always clearly visible on the colourless coating.

Originally all four plates were removed from the salt solution, rinsed with slow running water for 60 seconds to remove any dissolvable salt residue, and then furnace dried at 105°C for 15 minutes before being weighed on a daily basis. However after 120 hours some of the heavily build up corrosion crystals also started breaking off during the rinse and impeding the visual observations; therefore it was decided to no longer rinse the samples.

EDX measurements of the corrosion residue scraped from the surfaces of both samples indicated that the white crystals were predominantly an oxidized form of aluminium mixed with some sodium chloride. With the only apparent difference being the presence of fluorine in the corrosion product from the PVCC coating as a result of LiF being used during the coating process. XRD analysis confirmed that the corrosion product being formed was aluminium oxide generated by the disintegration of the primary aluminium layer underneath the conversion coatings. Considering the polarization curve of the PVCC coating this is no surprise as the corrosion potential of the coating is more positive than that of aluminium, but still more negative than that of the high strength steel (Figure 6.4-4).

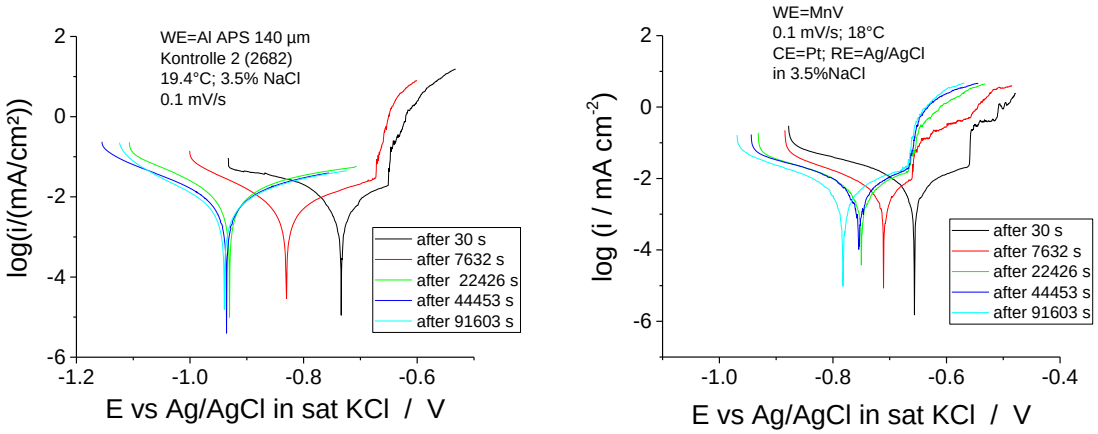

Figure 6.4-4: Anodic polarization curves after 25 hours for APS aluminium (left) and the Mn-V conversion coating (right).

Hexavalent chromium based coatings on the other hand has a corrosion potential slightly more negative than pure aluminium, and will corrode away preferentially instead of the primary aluminium coating. Unfortunately no polarization data was available for the Cr^{III}-Zr based commercial coating, but results clearly indicate that the corrosion potential of the coating is also more positive than that of the aluminium layer underneath which was corroded away to a greater extent than the surface coating.

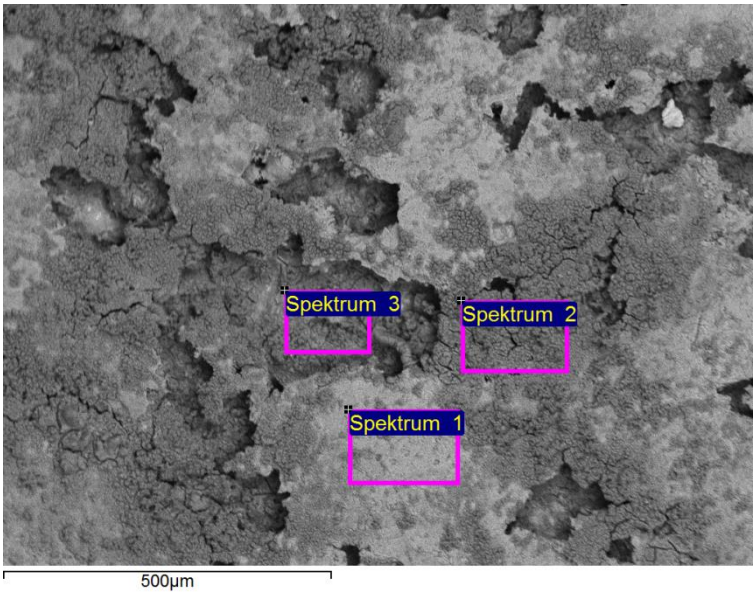

Figure 6.4-5: Backscatter electron image of the control coating after the 336 hour salt bath submersion test.

Table 6-2: EDX elemental mass % measurements of the areas indicated above in figure 6.

Elements	O	Na	Al	Si	S	Cl	Ca	Ti	V	Fe	Zr	Sum
Spectrum 1	29,3		66,0			2,1				0,3	2,2	100
Spectrum 2	62,4		30,5		0,4	6,0			0,2	0,6		100
Spectrum 3	56,0	0,3	36,5	0,2		0,4	0,7	0,4		5,4		100

As displayed in figure 6.4-5 above, the post exposure SEM EDX analyses indicated that the lighter areas still contained some zirconia from the passivation treatment. The dark areas on the other hand appear to consist mostly of aluminium oxide, and showed no traces of any chromium or zirconia anymore. Also evident when considering the subsurface APS aluminium was that it was readily corroded away beneath the Cr^{III}-Zr top layer allowing the remaining pieces of coating to be easily detached from the substrate during a tape adhesion test on half the sample (Figure 6.4-6).

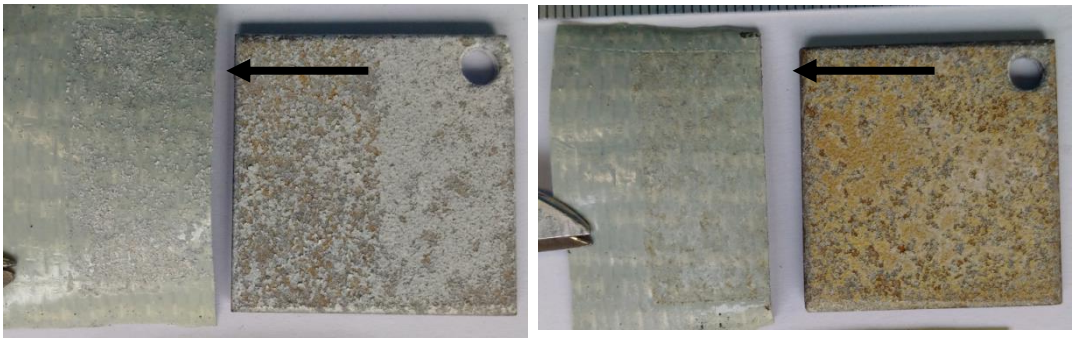

Figure 6.4-6: Adhesion tape test results of the SurTec650 plate (left) and the PVCC plate (right) after 336 hours of submersion.

In comparison analyses of the PVCC coated plate indicated that the substrate aluminium was still present beneath the remaining pieces of coating, and still

adhering to the substrate (Figures 6.4-7). A tape adhesion test of half of the sample surface confirmed this, as it could not detach the coating.

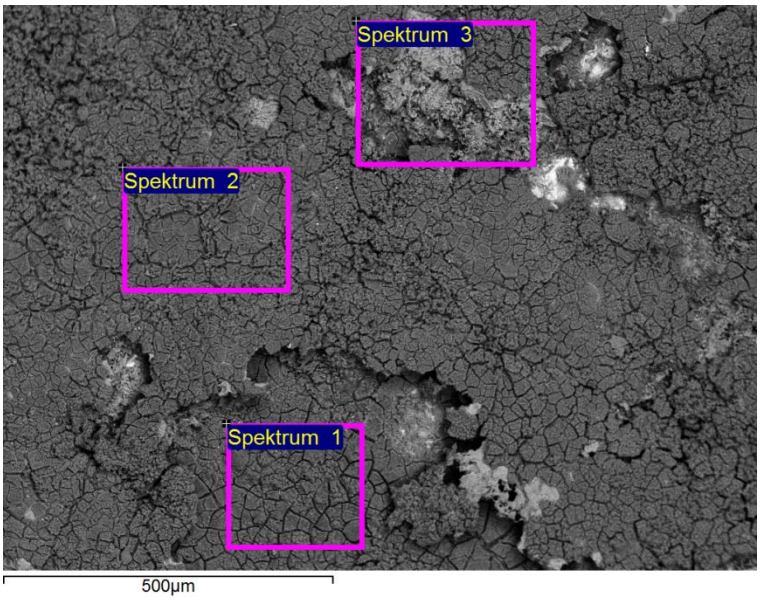

Figure 6.4-7: Backscatter electron image magnification of the PVCC coating after the 336 hour salt bath submersion test.

Table 6-3: EDX elemental mass % measurements of the areas indicated above in figure 6.4-7.

Elements	O	Na	Al	Si	S	Cl	Ca	V	Mn	Fe	Sum
Spectrum 1	64,24	0,24	30,71			1,27	0,15			3,38	100
Spectrum 2	62,61		34,54	0,2	0,24	0,48	0,1	0,34	1,05	0,43	100
Spectrum 3	52,86		44,9	0,11	0,14	0,78		0,2	0,6	0,4	100

Before the adhesion tape tests were done, with only the white corrosion product gently removed, the final weight loss measurements indicated that the PVCC coating did perform better but by a smaller margin than expected. The reason for this appeared to be shielding of the control sample surface with built up corrosion residue, as the initial corrosion rate was very high but slowed down once the entire surface was covered. The PVCC plate on the other hand appeared to corrode more slowly but at a consistent rate as the distribution of the corrosion crystals were more localized and did not at any time during the test cover the entire surface of the sample.

Table 6-4: Final weight loss of samples after the 336 hour salt bath submersion test.

Surface Treatment	**PVCC**	**Cr^{III}-Zr**
% Weight lost	0,32	0,42

Overall the corrosive environment of the agitated salt bath solution was evidently severe and resulted in highly accelerated corrosion of the two samples, and no doubt also influenced the mechanism of corrosion for both types of coatings. The end results did nonetheless indicate that under these circumstances the sacrificial corrosion protection offered by the PVCC coating was slightly better than that of the

commercial coating. In addition to this the tape test also indicated that the PVC coating remained better attached to the underlying aluminium substrate, with less of the underlying aluminium having corroded away.

The photos shown as figures 6.4-8 and 6.4-9 were taken of older experimental test samples created during the development of the PVCC coating that were submerged in salt water for 45 days under less severe conditions and then subjected to a tape test. For the first 2 days the solution was continuously stirred and aerated, and for the following 43 days the sample was left in the salt solution without agitation and only natural aeration which resulted in a much slower corrosion rate than that of the first 2 days. Nevertheless, the adhesion remained unaffected and the probes passed the tape test without difficulty (The black area on the surface of sample N is glue that remained behind from the aluminium conduction tape that was attached to the plate during a previous SEM analysis, and was not removed as it could have resulted in damage to the coating). Both the passivation and aluminium coatings were in much better condition, with no red rust visible on any of the samples and the coatings still solidly adhered to the substrate.

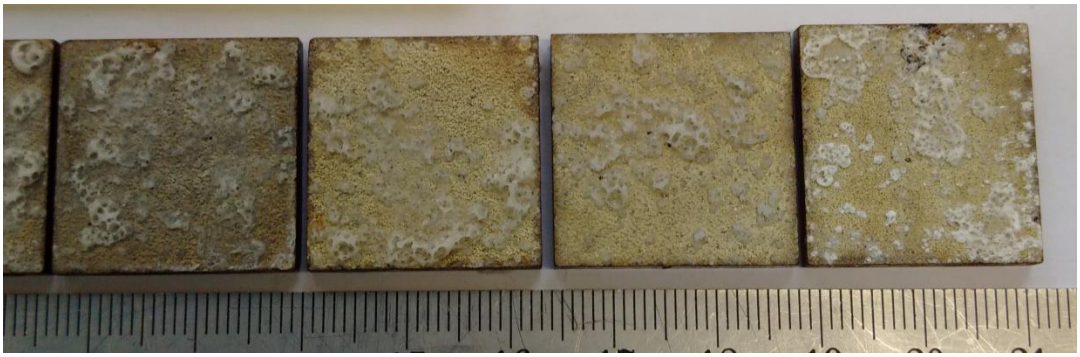

Figure 6.4-8: Samples I, K, M and N after 45 days in a naturally aerated 5 mass % salt solution.

Figure 6.4-9 : Results of the tape adhesion test for samples N and M, showing the coating still strongly adhering to the aluminium substrate after 45 days in a 5 mass % NaCl solution.

6.5 Corrosion results of the scribed plates

During the salt bath test of these four samples the two commercial control plates corroded at comparative rates as was expected. The corrosion rate of the two PVCC plates was however significantly different, with the scribed sample corroding much faster over the entire surface. This appeared to stem from the fact that the scratched

plate had a somewhat different geometry from the rest due it being a replacement plate. The other 3 plates were manufactured as 3 x 3 cm plates, and had their edges rounded before being APS coated with aluminium. The fourth plate in contrast was cut from a larger plate that had already been coated as the stock of smaller plates was depleted. The edges of this plate could not be rounded without damaging the aluminium coating (Figure 6.5-1).

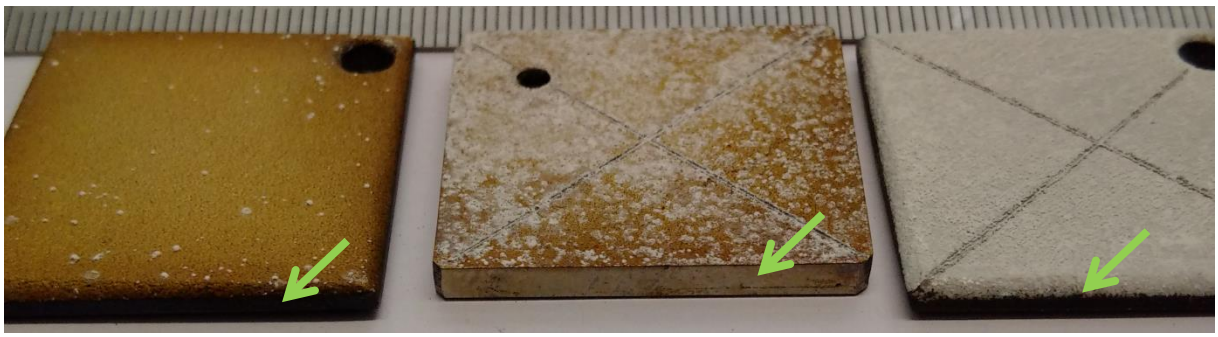

Figure 6.5-1: Passivated and un-passivated condition of steel substrate on samples with round and straight edges.

During the conversion coating process a layer of scale built up on the exposed steel edges, and remained in place throughout the corrosion test if the edges were rounded. However, it was noted that for the scribed PVCC plate with vertical edges all the scale had detached from the sides and exposed far more steel to the solution than the scratched section was indented to do. Figure 6.5-2 illustrates how the scale layer covering the steel flaked off from the surface if the side of the sample was not rounded before APS coating. The 336 hour salt bath corrosion test was therefore repeated using another plate that had two straight sided edges but covered with tape this time. (Figures 6.5-3 & 6.5-4)

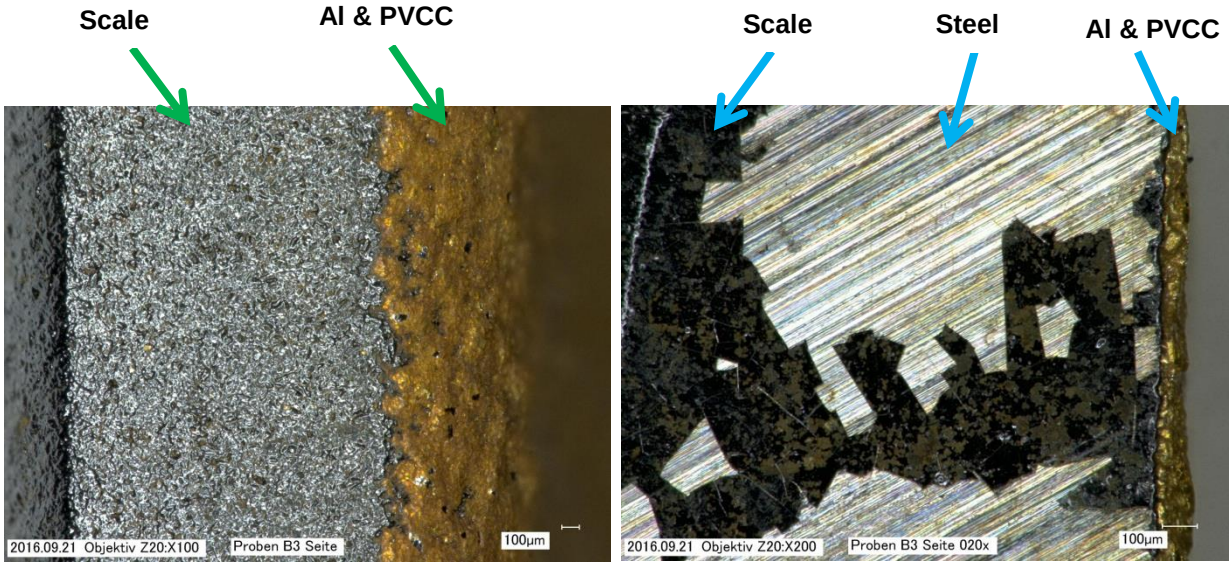

Figure 6.5-2: Images indicating how the scale remained on the curved edge sample on the left compared to the disintegration on straight edges to expose the steel substrate on the right.

Again up until 120 hours of submersion the samples were still washed to remove any soluble sodium chloride crystals before being weighed, however after that in order to prevent some of the oxide/hydroxide also becoming detached the practice was stopped with only the difference between the initial and final weights of the sample used to calculated the weight loss.

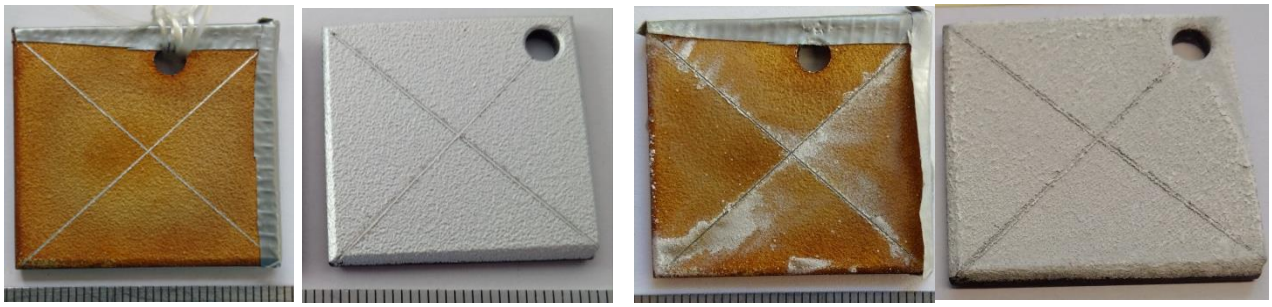

Figure 6.5-3: The scratched samples at 0 hours (left) and after 24 hours (right) of submersion.

Figure 6.5-4: On the left are the scratched plates after 144 and 120 hours respectively, and both after 336 hours on the right.

Table 6-5: Final weight loss measurements of scribed samples after the 336 hour salt bath submersion test.

Surface Treatment	**PVCC**	**Cr^{III}-Zr**
% Weight lost	0,33	0,54

The corrosion results of the scratched plates closely mimicked that of the undamaged plates with the PVCC plate clearly displaying a slower rate of corrosion during the early stages, but the advantage became less distinguishable closer to the end of the test as the surfaces of both plates had become almost entirely covered with the corrosive product. A small noticeable difference between the two samples was that corrosion on the PVCC plate had initially been concentrated in the region adjacent to the scratch and gradually spread across the entire surface, while for the control plate the corrosion showed no preference for initiating at the damaged area. In terms of weight lost, the scribe had very little influence on the PVCC plate with an increase of only 0,01% in mass loss while the control sample lost an additional 0,12% compared to the un-scribed plate.

6.6 Active passivation protection

What is interesting to note regarding the PVCC sample that was initially corroded with 4 open sides is that the steel surfaces appeared to have been passivated during the test. Initial photographs show the silver colored steel surface to be clearly visible after the scale detached. However while taking weight measurements it was noted that the sides appeared golden. Under magnification it can be seen that the golden surface contained some dendritic crystals, which would indicate that the coating grew on top of the steel and is not merely the result of surface corrosion (Figures 6.6-1 & 6.6-2).

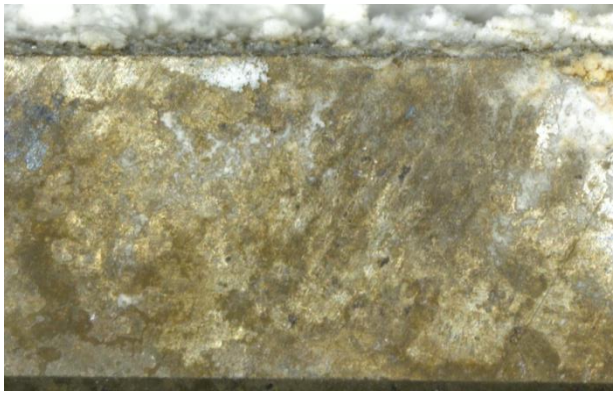

Figure 6.6-1: Side on image at approximately 50x magnification of the open sided PVCC plate after 336 hours of submersion.

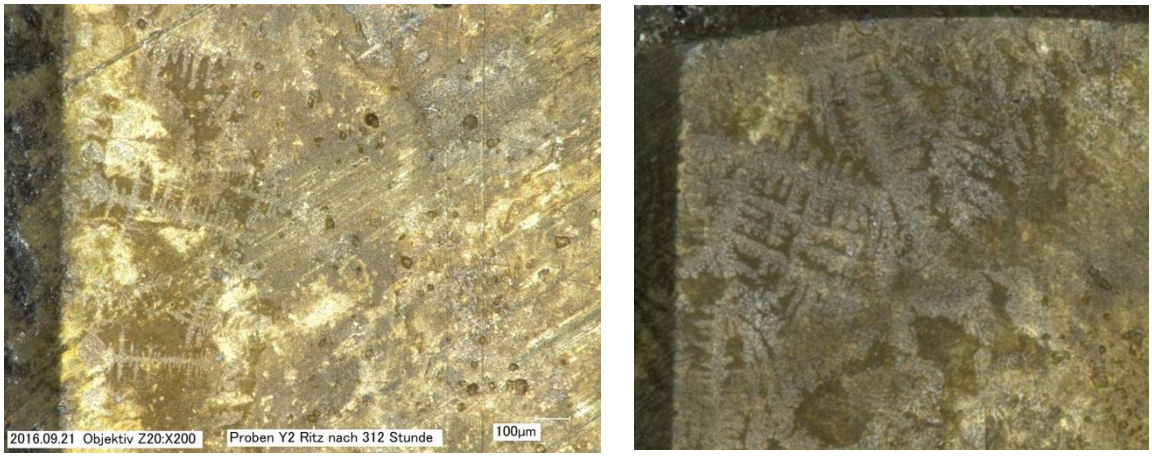

Figure 6.6-2: Side on images at approximately 200x (left) and 100x (right) magnification showing the dendritic crystal growth of the coating on the adjacent open steel sides

SEM inspection and EDX analysis of the steel surface indicated that the golden phase consist of aluminum and vanadium, but likely little to no manganese as the quantity measured differed little from that present in the steel itself (Figures 6.6-3). The phase is also different from the white corrosion product scraped off the samples which did not contain any measureable quantity of vanadium. This active passivation behaviour explains why the scribe had so little influence on the corrosion rate of the PVCC plate as the weight loss measurements obtained for both the plain and damaged samples were practically identical, which is highly unusual.

Figure 6.6-3: Backscatter electron image of the golden layer than forms on the open steel sides during the corrosion test.

Table 6-6: EDX elemental mass % measurements of the areas indicated in figure 9 above.

Elements	O	Na	Mg	Al	Si	Cl	Ca	V	Cr	Mn	Fe	Sum
Spektrum 1	6,67	0,4		0,71	0,33				1,18	0,74	89,98	100
Spektrum 2	18,19	0,79	0,26	4,53	0,28		0,21	0,23	0,9	0,69	73,92	100
Spektrum 3	18,5	1,04	0,31	3,26	0,32	0,18	0,34	0,31	0,96	0,85	73,93	100

6.7 Neutral Salt Spray Test

Due to the limited availability of the neutral salt fog chamber no further testing or refining of the coating solution could be done, and the procedure was scaled up for the coating of two larger 10 x 15 cm plates, using the same solution and parameters as for sample Y, with the exception of the LiF, of which a concentration of 0.5 g/l was used instead of 0.8 g/l as a result of a mistake made during the weighing of the salts. These two plates along with two commercial control samples coated with *Surtec650 chromitAl* (colorless) were then sent to Ilmenau Technical University for a 500 hour ISO 9227 neutral salt spray corrosion test. As can be seen in figure 6.7-1 the aluminium layer on one plate of each set was again scribed to expose the underlying steel and enable both barrier and sacrificial properties to be investigated.

Table 6-7: Processing parameters of 10x15 cm plates PVCC coated for the neutral salt fog test.

Sample	Substrate	pH	Time (min)	Hot alkaline etch (min)	$KMnO_4$ (g/l)	$NaVO_3$ (g/l)	$NaNO_3$ (g/l)	LiF (g/l)
NSS test plates	**Al on 42CrMo4**	11	30	1.5-2	20	10	4	0.5

Figure 6.7-1: Plates coated for NSS testing, PVCC (left) and *SurTec650 chromitAL* (right).

Depending on the institution at which the neutral salt spray test is conducted the plates are either placed in a standing rack at a 20° angle or hanged vertically, both options are allowed in ASTM B117 / ISO 9227 specifications. At the Technical University of Ilmenau the plates were hanged using nylon wire and therefore required a hole to be drilled at one end. A second hole was also drilled at the opposite end as it was required for the level suspension of the plate during the coating process. As can be seen in figures 6.7-2 to 6.7-5 the holes and the area surrounding them were sources of red rust formation on all four of the tested plates, but still remained within the exclusion zone of 1 cm from the sides. Initially the plates were placed in the salt fog chamber in the as received condition for the first day, but there was some concern regarding possible influence of streaks of iron corrosion product that might be generated on the top and at the sides, and it was decided to rather seal off the steel surfaces of the samples with isolating tape.

Figure 6.7-2: PVCC coated plate after 0, 25, 240 and 500 hours in a neutral salt fog chamber. (ASTM B117 / ISO 9227).

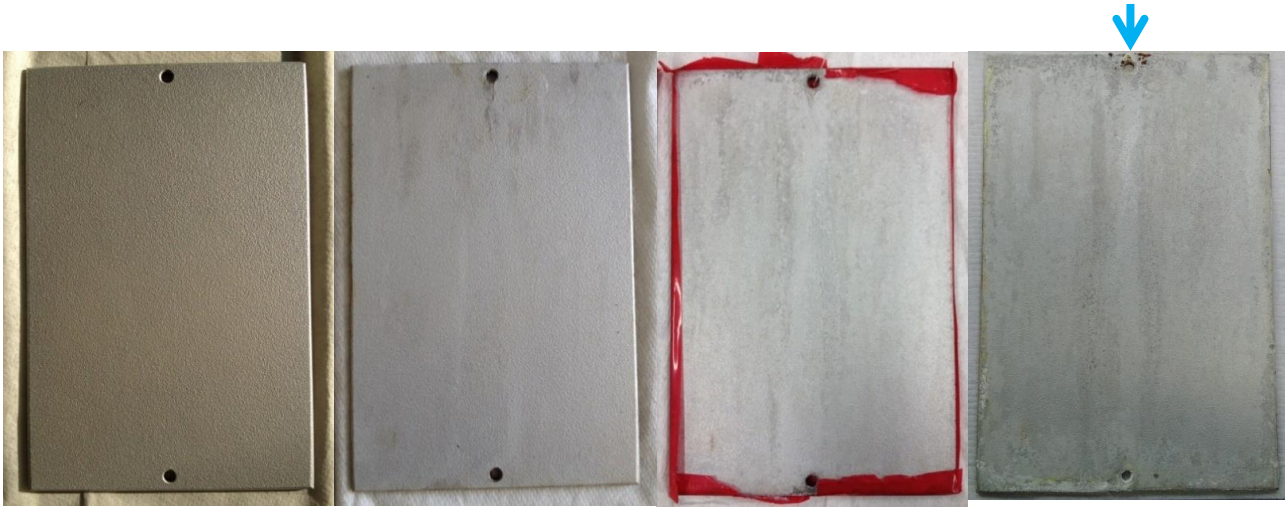

Figure 6.7-3: Cr^{III}-Zr coated plate after 0, 25, 240 and 500 hours in a neutral salt fog chamber. (ASTM B117 / ISO 9227)

The visual observations were somewhat hindered by the fact that the *SurTec650 chromitAl* coating was colourless, with the white corrosion streaks not contrasting clearly on the silver coloured surface, while with the PVCC coated plates the corrosion streaks were clearly visible. Nevertheless after 500 hours the centre sections of both un-scribed plates were still in good condition. Both had some rust formation around the top hole, more so for the PVCC plate, but not exceeding the exclusion zone. The performance of the two types of coatings could therefore not be separated as both successfully passed the required 336 hours, and in order to distinguish between their performances more tests with longer exposure times would be required.

Figure 6.7-4: Artificially damaged PVCC coated plate after 0, 25, 240 and 500 hours in a neutral salt fog chamber.

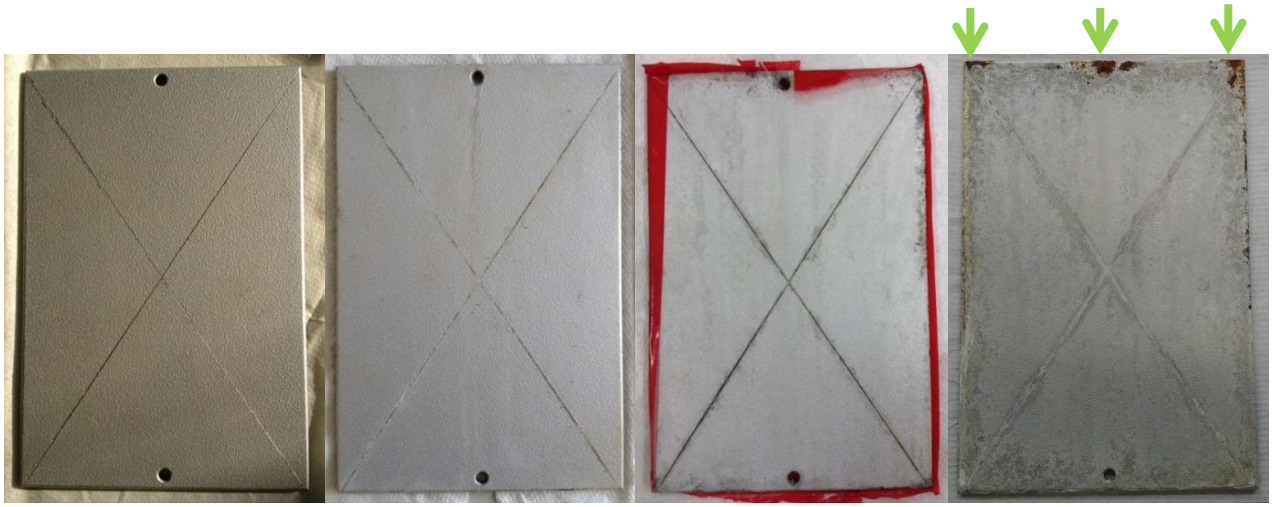

Figure 6.7-5: Artificially damaged Cr^{III}-Zr coated plate after 0, 25, 240 and 500 hours in a neutral salt fog chamber.

However when looking at the scribed samples the control plate had rust formation not only around the hole but also along the edges of the sample. The surface could also be seen to have deteriorated from the sides inwards to such an extent as to surpass the 1 cm exclusion zone. Similarly the central areas surrounding the scribe could also be seen to have deteriorated more rapidly. In comparison it was clear that the areas surrounding the scribe on the PVCC plate displayed little indication of accelerated corrosion. This might be due to the active passivation effect the coating exhibited during the submersion test were a new vanadium rich dendritic crystal layer was found to grow onto adjacent open steel surfaces.

Overall when considering only barrier protection both coatings displayed satisfactory corrosion resistance in the salt fog chamber, with no clear separation possible. When taking into account the sacrificial corrosion protection of the two coatings the PVCC endured slightly better than the commercial control sample in this test. Unfortunately the sample size of the trial was too small for a definitive outcome, but when also taking the salt bath results into consideration, there is a strong indication that the experimental permanganate-vanadate based coating surpasses the Cr^{III}-Zr based coating in sacrificial protection.

6.8 Improved coating times

After the salt bath submersion and neutral salt spray tests yielded some positive results, indicating that the PVCC coating compared well against an industrial reference, it was decided to try and decrease the coating's reaction time down into the 3-5 minute range for it to be more commercially suitable. This would allow the solution to be used as a drop in replacement for hexavalent chromium, without having a negative influence on the production rate of the chemical processing line.

Table 6-8: Coating parameters used to produce samples with shorter processing times.

Sample	pH	Time (min)	Alkaline etch (min)	$KMnO_4$ (g/l)	$NaVO_3$ (g/l)	$NaNO_3$ (g/l)	LiF (g/l)	H_2O_2 (g/l)	H_3PO_4 (g/l)
A1	11	3	0.5-1	20	10	4	0.5	2.5	0
A2	11	5	0.5-1	20	10	4	0.5	2.5	0
A3	11	10	0.5-1	20	10	4	0.5	2.5	0
B1	11	3	0.5-1	20	10	4	0.5	5.0	0
B2	11	5	0.5-1	20	10	4	0.5	5.0	0
B3	11	10	0.5-1	20	10	4	0.5	5.0	0
C1	9	10	0.5-1	20	10	4	0.5	5.0	8
D1	11	3	0.5-1	20	10	4	0.5	5.0	16

Initially the original solution was used, but with the addition of hydrogen peroxide at a concentration level of 2,5 g/l to act as an additional strong oxidant, and the sample plates coated for 3, 5 and 10 minutes. All rinsing and pre-treatment stages remained unchanged, and the pH was maintained in the buffer region of 11. Next the H_2O_2 concentration was further increased to 5 g/l and another three samples were again treated for 3, 5 and 10 minutes, respectively.

Following this phosphate was introduced into the coating bath through the addition of phosphoric acid. At a concentration of 8 g/l the solution pH decreased down to 9, at which a single sample was coated for 10 minutes after inspection at the 3 and 5 minute intervals indicated that the solution did not produce adequate coatings. Sodium hydroxide was again used to raise the solution pH back up to the buffering region of pH 11. Once more a sample plate was coated for 3 minutes and emerged with a dark purple-brown coloured coating.

All eight test samples were left to dry and cure for 2 days after which each were microscopically inspected and subjected to a tape test in order to measure the level of adhesion to the substrate. All of the samples contained some loose deposits or residue on the surface that were not part of the coating, however only samples which were treated for 3-5 minutes using only additional hydrogen peroxide in the solution (A1, A2, B1 and B2) showed no damage of the underlying golden coloured coating. The conversion coating of the other 4 samples treated for longer times or containing phosphoric acid all sustained some damage after the tape was removed (Figure 6.8-1 & 6.8-2).

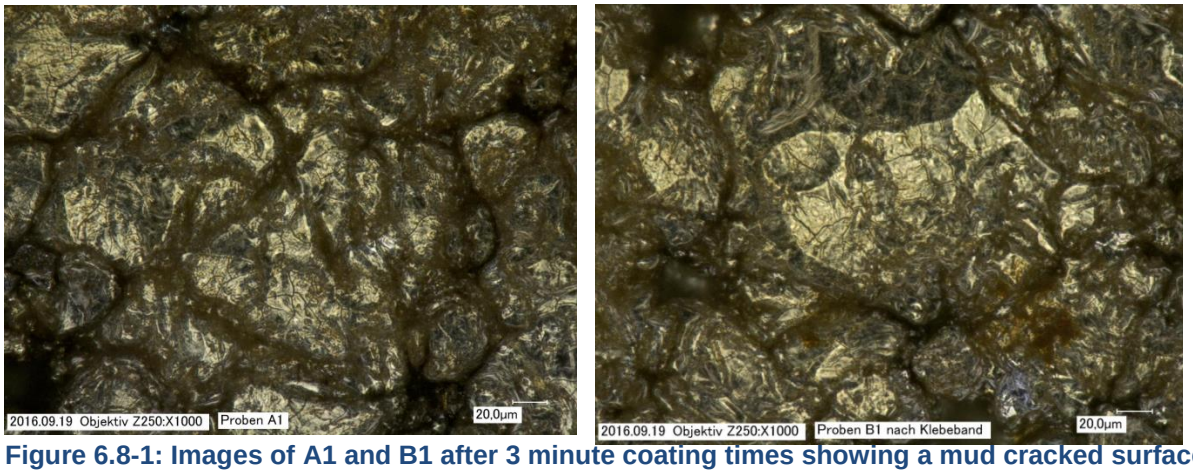

Figure 6.8-1: Images of A1 and B1 after 3 minute coating times showing a mud cracked surface with no damage the tape test. (Approximately 1000x magnification)

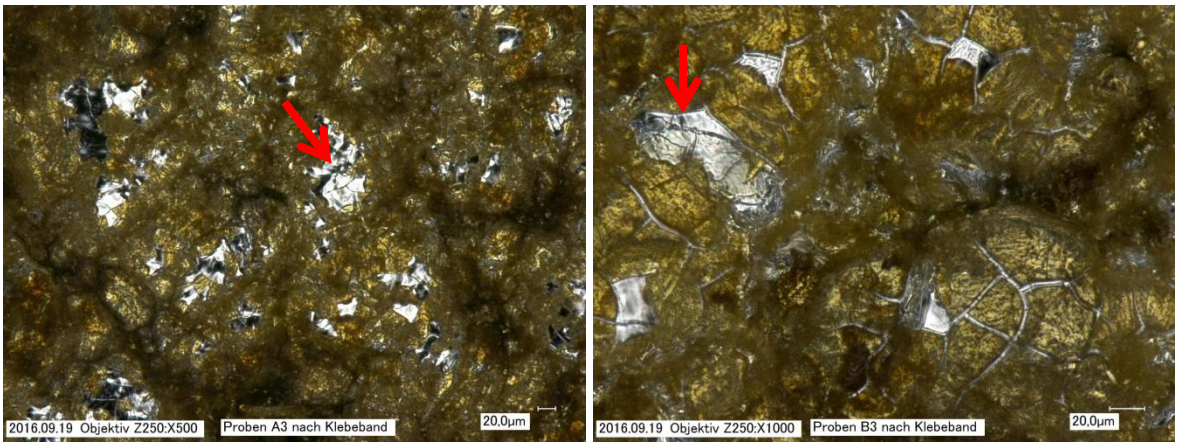

Figure 6.8-2: Images at approximately 500x (left) and 1000x (right) magnification of A3 and B3 coated for 10 minutes and damaged after being subjected to the tape test.

As the neutral salt spray chamber was no longer available to conduct another test to find out whether the improved coating with a commercially suitable reaction time could still pass the specified level of corrosion resistance, the coating was again tested in the laboratory scale salt bath setup as described previously. For comparison with the 30 minute coating two 2 x 2 cm sized plates were coated using a concentration of 2,5 g/l hydrogen peroxide, similar to that of sample A1, and two 3 x 3 cm plates coated for 30 minutes using the original stock solution, as described for sample C in Table 6-1 above. As the sample edges were not rounded the back and sides of all four samples were closed off with tape before submersion.

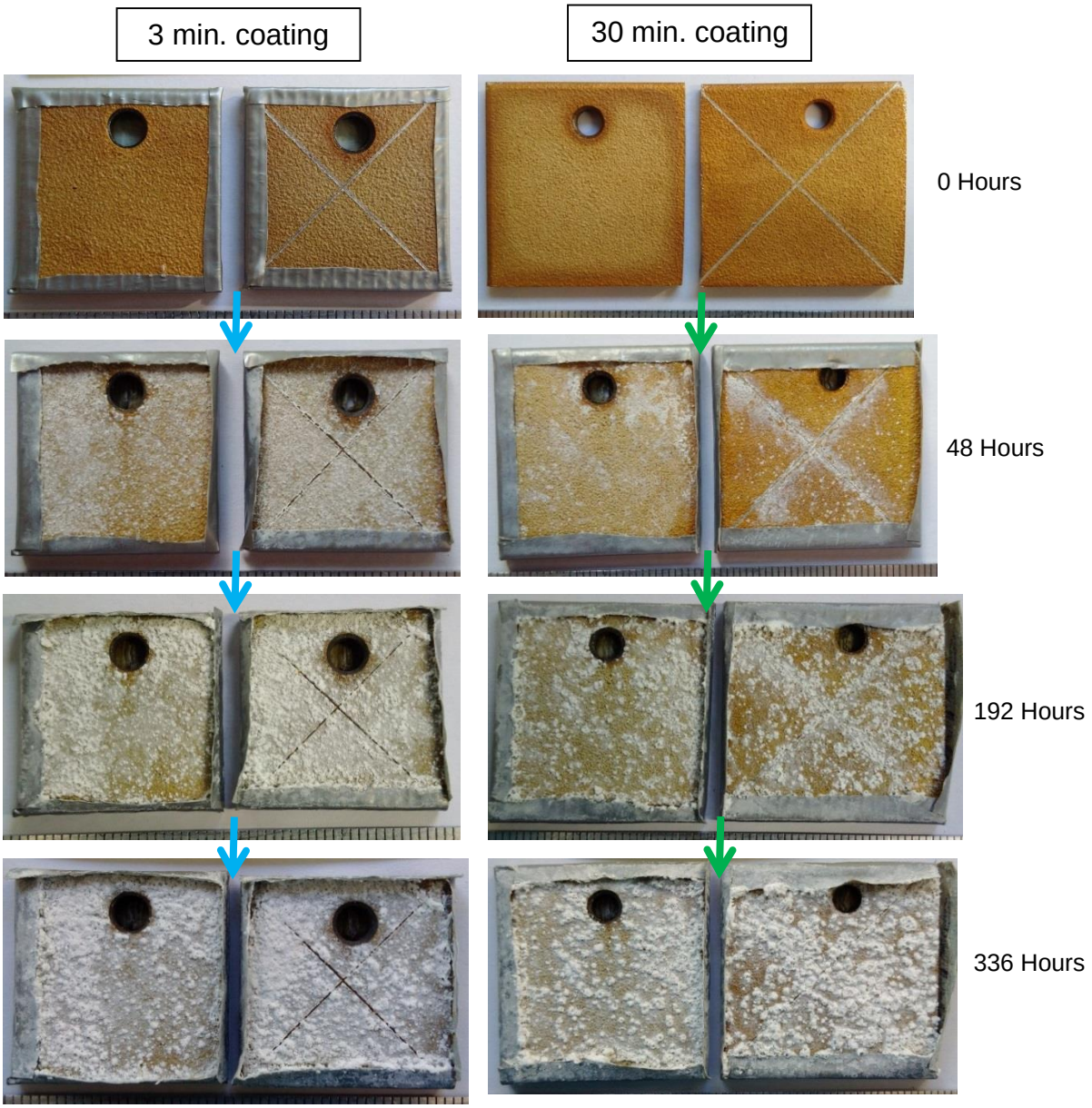

Figure 6.8-3: Comparison of 3 minute and 30 minute coatings during 336 hours submersion in a 5 mass % NaCl solution.

Table 6-9: Weight loss of PVCC coated samples after 336 hours salt water submersion test.

	% Weight loss	
Surface treatment	**Plain**	**Scribed**
3 min. PVCC	0,06	0,06
30 min. PVCC	0,03	0,07

During the first few days of submersion the build-up of corrosion product was more widespread over the surface of the 3 minute samples, with final weight measurements indicating double the weight loss for the un-scribed samples (Figure 6.8-3). The weight lost by the two scribed samples was very similar, but this might be due to the tape detachment that occurred on one side of the 30 minute sample that would have had a negative effect on the corrosion rate. Nevertheless the 3 minute coating does seem to be able to still provide a reasonable level of protection and

might become a viable commercial product if it can do well in the other required tests such as neutral salt spray, and base coat paint adhesion.

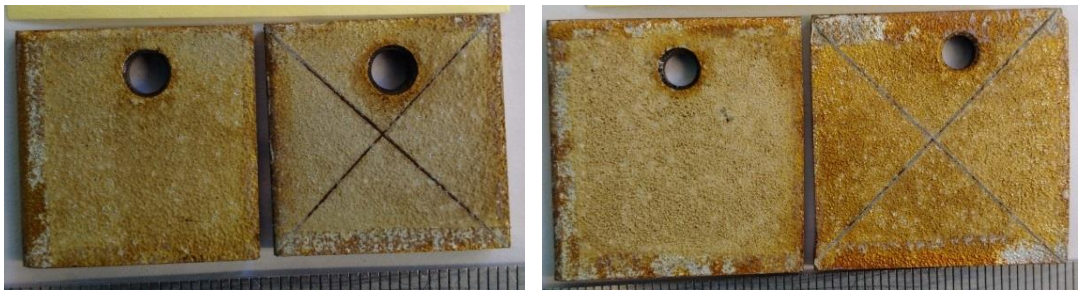

Figure 6.8-4: Coating condition after 336 hours with the white corrosion product removed.

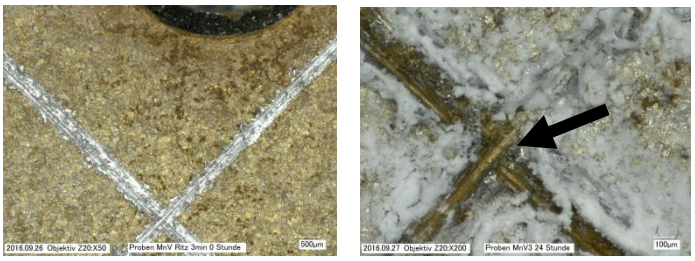

Figure 6.8-5: Surface images of the scratched 3 minute PVCC plate after 0 and 24 hours of submersion.

After the tape and corrosion product was removed from the test samples the coatings still appeared to be in a relatively good condition with the dark markings inside the scribe not being rust but rather the result of the active passivation also displayed during previous tests (figure 6.8-4). Note also in figure 6.8-5 above how the exposed surface inside the scribe on the 3 minute coating was overgrown with a vanadium rich layer within 24 hours after submersion.

7 Part B Conclusion

The Mn-V based conversion coating appears to hold much promise as a possible alternative to Cr^{VI} based coatings. Other than being less hazardous than chromate, and therefore not affected by European REACh regulation, it has:

- Standard processing steps and a reaction time of 3 minutes which would allow it to be used as a drop-in replacement on industrial processing lines without requiring any modification to the facilities or production schedule.
- It has a golden colour similar to that of chromate conversion coatings, which unlike the Cr^{III}-Zr coating, enables the line operators to do visual quality control inspections during processing.
- Whenever damaged it readily forms a protective passivation layer on any exposed steel.

There are however still numerous other tests that the coating needs to be put through, the most important of which is paint adhesion as the majority of conversion coated surfaces are covered with basecoat paint. Therefore it is absolutely critical that there is good adhesion between the two. Further refinement of the coating solution to find the optimum Mn:V ratio could possibly result in these types of Mn-V based coatings becoming an attractive alternative as a possible Cr^{VI} replacement.

8 Recommended future work

For the thermally sprayed Al-Mn alloy it is recommended that:

- Its ability to coat components with geometries more complex than plate be investigated.
- Long term ISO 9227 corrosion tests in the 1000-3000 hour range be conducted.
- The pre-treatment stages required for conversion coatings of the alloy be finalised.
- Investigate whether it has any significant advantage over pure aluminium in terms of pitting corrosion and hydrogen re-embrittlement.
- Try to improve the adhesion of the alloy for bend test requirements.

Lastly for the Mn-V conversion coating it is recommended that:

- The Mn:V ratio be optimised to give the best possible corrosion resistance.
- Long term ISO 9227 corrosion test be done.
- Processing pre-treatment stages modified to allow successful coating of aluminium alloy 2024-T3 and other commonly used aluminium alloys.
- Base coat paint adhesion tests be conducted.

9 Acknowledgements

There are many people without whose generosity, patience, knowledge and selfless contribution this project would not have been possible. Firstly I would like to thank Andrea Förg for giving me the opportunity of working on project Alti2de. I am also very grateful to Russel Grefen for giving me the opportunity of working at Aerosud Aviation, and my colleagues there, Jan, Darnell, Buchhardt and Onika for teaching me everything about the manufacturing of aircraft components. I would also like to thank everybody at Fraunhofer UMSICHT with whom I had the privileged of working with, Gerhard, Angelika, Ingrid, Klaus, Gunther and Christina. Also Boris Butschies at SurTec for generously supplying the control samples and Laure at CRM for the cadmium test results. Lastly a special thanks to Dokterin Adriana Ispas at TUI for the input and assistance she provided during this project. The financial assistance of the National Research Foundation (NRF) towards this research is hereby acknowledged. Opinions expressed and conclusions arrived at, are those of the author and are not necessarily to be attributed to the NRF. This work has been performed at Fraunhofer UMSICHT in Sulzbach-Rosenberg, Germany, as part of a transnational CORNET project with the IGF project no. 104 EBG and with the financial support by the German Ministry of Economics and Energy based on a decision of the German Bundestag.

10 References

[1] http://echa.europa.eu, visited on 11 May 2016.05.12

[2] M. Bielewski, *Replacing cadmium and chromium*, in: *Corrosion Fatigue and Environmentally Assisted Cracking in Aging Military Vehicles*, NATO Report no. RTO-AG-AVT-140, published in 2011, ISBN 978-92-837-0125-5, pp. 23.1-23-22.

[3] CORNET proposal for project Alti2de, *Alternative coatings to cadmium and hard chromium with potential for second generation developments*, October 2012, pp1-57.

[4] G. Holmbom (CSM Materialteknik), E. Hultgren (SAAB), Presentation: *Experience on Cadmium Replacement at Saab Aerospace*, 2005.

[5] https://www.niehs.nih.gov/health/materials/cobalt, last visited 11.08.2017.

[6] http://www.OSHA.gov. visited 16 May 2016.

[7] http://www.OSHA.europa.eu/de. visited 16 May 2016.

[8] E. Beck, J. Green, S. Brown, C. Richards, E. Duffy, *Final Report: Aluminum Manganese Molten Salt Plating WP 9903*, Naval Air Systems Command, Materials Engineering Division, Patuxent River, Maryland, June 2006.

[9] M.C. Reboul, B. Baroux, *Metallurgical aspects of corrosion resistance of aluminium alloys*, Materials and Corrosion, 2011, Volume 62(3), pp. 215-233.

[10] http://www.compositesworld.com, visited on 30 May 2016.

[11] http://www.airbus.com, visited on 30 May 2016.

[12] U. Donatus, G.E. Thompson, Z. Lui, *Study of the Effect of Cadmium on the Bimetallic Corrosion Behavior of AA2024T3 and Mild Steel Couple*, Journal of Materials Engineering and Performance, 2015, Volume 24(5), pp. 1897-1905.

[13] D. Figueroa, M.J. Robinson, *The effects of sacrificial coatings on hydrogen embrittlement and re-embrittlement of ultra high strength steels*, Corrosion Science, 2008, Volume 50, pp.1066-1079.

[14] A. Ross, D. Aylor, *Cadmium replacement alternatives for corrosion and hydrogen embrittlement protection of high strength steels*, Naval Surface Warfare Center, DoD Corrosion Conference 2009.

[15] A. Conde, M.A. Arenas, J.J. de Damborenea, *Electrodeposition of Zi-Ni coatings as Cd replacement for corrosion protection of high strength steel*, Corrosion Science, Volume 53, 2011, pp. 1489-1497.

[16] A.D. Zhirnov, S.A. Karimova, L.V. Ovsyannikova, O.A. Gubenko, *New protective coatings for replacing cadmium coatings on steel parts*, Metal Science and Heat Treatment, 2003, Volume 45, pp. 23-25.

[17] M.J. Kane, C. Matzdorf, J. Green, E. Beck, *Evaluation of Aluminum-Manganese as a Cadmium Replacement*, Surface Modification Technologies 2002, Volume 15, pp.265-273.

[18] S. S. Vinogradov, 1998, *Ecologically Safe Galvanic Production*, Globus, Moscow, pp 7-13.

[19] A. Agüero, J.C. del Hoyo, J.G. de Blas, M. García, M. Gutiérrez, L. Madueño, S. Ulargui, 2012, *Aluminiun Slurry Coatings to Replace Cadmium for Aeronautical Applications*, Surface Coating Technology, Volume 213, pp.229-238.

[20] K. Legg, "*Cadmium Replacement Options*", presented to The Welding Institute, Cambridge, UK, October 2003.

[21] M. Reffass, C. Berziou, C. Rébéré, A. Billard, J. Creus, *Corrosion behavior of magnetron-sputtered Al1-x-Mnx coatings in neutral saline solution*, Corrosion Science, 2010, Volume 52, pp. 3615-3623.

[22] http://www.chemistry.mcgill.ca/msds/, last visited 15.08.2017.

[23] http://www.sciencelab.com/msds, last visited 15.08.2017.

[24] T.P. Moffat, G.R. Stafford, D.E. Hall, *Pitting Corrosion of Electrodeposited Aluminium-Manganese Alloys*, Journal of Electrochemical Society (1993), pp. 2779-2786.

[25] S. Ruan, C.A. Schuh, *Electrodeposited Al-Mn alloys with microcrystalline, nonocrystalline, amorphous and nano-quasicrystalline structures*, Acta Materialia, 2009, Volume 57, pp.3810-3822.

[26] J. Reyes-Gasga, G. Mondragon-Galicia, M. José-Yacamán, *In-situ transmission electron microscopy observation of the phase transformation in thin films of the Al-Mn system*, Thin Solid Films, 1992, Volume 227, pp. 24-31.

[27] J. Zhang, C. Yan, F. Wang, *Electrodeposition of Al-Mn alloy on AZ31B magnesium alloy in molten salts*, Applied Surface Science, 2009, Volume 255, pp. 4926-4932.

[28] J.C. Li, S.H. Nan, Q. Jiang, *Study of the electrodeposition of Al-Mn amorphous alloys from molten salts*, Surface Coating Technology, 1998, Volume 106, pp. 135-139.

[29] Y. An, X. Zhao, G. Hou, H. Zhou, Je Chen, Jianmin Chen, *Tribological and Thermal Properties of Mullite Coating Prepared by Atmospheric Plasma Spraying*, Journal of Thermal Spray Technology, 2013, Volume 23 (3), pp. 410-419.

[30] W. Lauwerens, A. De Boeck, M. Thijs, S, Claessens, M. Van Stappen, P. Steenackers, *PVD Al-Ti and Al-Mn coatings for high temperature corrosion protection of sheet steel*, Surface and Coating Technology, 2001, Volume 146-147, pp. 27-32.

[31] Z. Yin, S. Tao, X. Zhou, *Effect of the thickness on properties of Al_2O_3 coatings deposited by plasma spraying*, Materials Characterization, 2011, Volume 62, pp. 90-93.

[32] W. Laurens, A. Boeck, M. Thijs, S. Claessens, M. Van Stappen, P. Steenackers, *PVD Al-Ti and Al-Mn coatings for high temperature corrosion protection of sheet steel*, Surface and Coating Technology, 2001, Volume 146-147, pp.27-32.

[33] T. Lui, J. Arnold, *Study of in-flight particle stream and particle behavior for understanding the instability phenomenon in plasma spraying process*, Surface and Coating Technology, 2016, Volume 286, pp. 80-94.

[34] K. Bobzin, N. Kopp, T, Warda, I. Petkovic, S. Zimmermann, K. Hartz-Behrend, K. Landes, G. Foster, S. Kirner, J.L. Marques, J. Schein, J. Prehm, K. Möhwald, Fr.W. Bach*, Improvement of Coating Properties in Three-Cathode Atmospheric Plasma Spraying, Journal of Thermal Spray Technology*, 2013, Volume 22(4), pp. 502-508.

[35] J.F. Bisson, B. Gauthier, C. Moreau, *Effects of plasma fluctuations on in-flight particle parameters*, Journal of Thermal Spray Technology, 2003, Volume 12, pp. 38-43.

[36] R.R. Kieschke, K.A. Roberts, T.W. Clyne, *Instabilities in the vacuum plasma spraying process*, Surface Coating Technology, 1991, Volume 46, pp.25-38.

[37] S. Fokeer, S. Kingman, I. Lowndes, A. Reynolds, *Characterisation of the cross sectional particle concentration distribution in horizontal dilute flow conveying-a review*, Chemical Engineering Processes, 2004, Volume 43, pp.677-691.

[38] M.L. Berndt, C.C. Berndt, Thermal Spray Coatings, *Corrosion: Fundamentals, Testing and Protection*, Volume 13A, ASM Handbook, ASM International, 2003, pp.803-813.

[39] M. Vreijling, *Electrochemical Characterization of Metallic Thermally Sprayed Coatings*, Ph.D Thesis, TNO Institute of Industrial Technology, The Netherlands, 1998.

[40] R. Arrabal, A. Pardo, M.C. Merino, M. Mohedano, P. Casajus, S. Merino, *Al/SiC thermal spray coatings for corrosion protection of Mg-Al alloys in humid and saline environments*, Surface Coating Technology, 2010, Volume 204, pp.2767-2774.

[41] S.A. Kulinich, M. Farzaneh, X.W. Du, *Growth of Corrosion-Resistant Manganese Oxide Coatings on an Aluminum Alloy*, Inorganic Materials, 2007, Volume 43(9), pp. 956-962.

[42] T.J. Warner, M.P. Schmidt, F. Sommer, D. Bellot, *Characterization of corrosion initiation on 2024 aluminium alloy by atomic force microscopy*, Zeitschrift für Metalkunde, 1995, Volume 86, pp. 494.

[43] M.C. Reboul, T.J. Warner, H. Mayet, B. Baroux, *A Ten Step Mechanism for the Pitting Corrosion of Aluminium Alloys* , Corrosion Reviews, 1997, Volume 15, pp. 471.

[44] J.W. Bibber, *Non-Chrome-Containing Conversion Coatings for Zinc and Zinc Alloys*, Metal Finishing, 2008, Volume 106(4), pp. 41-46.

[45] R.G. Buchheit, A.E. Hughes, *Chromate and Chromate-free Conversion Coatings, Corrosion: Fundamentals, Testing and Protection*, Volume 13A, ASM Handbook, ASM International, 2003, pp. 720-735.

[46] http://www.mansfield-anodisers.co.uk, visited 14 July 2016.

[47] L. Xia, R.L. McCreery, *Chemistry of a chromate conversion coating on aluminium alloy AA2024-T3 probed by vibrational spectroscopy*, Journal of Electrochemical Society, 1998, Volume 145, pp.3083-3089.

[48] P. Campestrini, E.P.M.V. Westing, J.H.W. deWit, *Influence of surface preparation on performance of chromate conversion coatings on alclad 2024 aluminium alloy: Part I: Nucleation and growth*, Electrochemica Acta, 2001, Volume 46, pp. 2553-2571.

[49] A. Katzman, G. Malouf, R. Bauer, G.W. Stupian, *Corrosion-protective chromate coatings on aluminium*, Applications of Surface Science, 1979, Volume 2, pp. 416-432.

[50] J. Zhao, G.S. Frankel, R.L. McCreery, *Corrosion Protection of Untreated AA-2024-T3 in Chloride Solution by a Chromate Conversion Coating Monitored with Raman Spectroscopy*, Journal of The Electrochemical Society, Volume 145, 1998, pp. 2258-2264.

[51] L. Xia, E. Akiyama, G. Frankel, R. McCreery, *Storage and Release of Soluble Hexavalent Chromium from Chromate Conversion Coatings Equilibrium Aspects of Cr^{VI} Concentration*, Journal of The Electrochemical Society, Volume 147, 2000, pp. 2556-2562.

[52] M.W. Kendig, A.J. Davenport, H.S. Isaacs, *The mechanism of corrosion inhibition by chromate conversion coatings from x-ray absorption near edge spectroscopy (Xanes*), Corrosion Science, Volume 43, 1993, pp. 41-49.

[53] Specification 9904151, U.S. Department of Energy, “Coating, Chromate on Aluminum”, 1989.

[54] K. Legg, *Cadmium Replacement Alternatives for the Joint Strike Fighter, Rowan Technology Group*, Libertyville, IL, USA, Report No. 3105JSF3, 18 December 2000.

[55] S. Pommiers, J. Frayret, A. Castetbon, M. Potin-Gautier, *Alternative conversion coatings to chromate for the protection of magnesium alloys*, Corrosion Science, 2014, Volume 84, pp.135-146.

[56] G. Yoganandan, J.N. Balaraju, *Synergistic effect of V and Mn oxyanions for the corrosion protection of anodized aerospace aluminum alloy*, Surface and Coatings Technology, 2014, Volume 252, pp. 35-47.

[57] E. Huttunen-Saarivirta, V.T. Kuokkala, H. Paajanen, *Corrosion effects of runway de-iceing chemicals on aircraft alloys and coatings*, Materials Chemistry and Physics, 2011, Volume 126, pp. 138-151.

[58] X. Zuo, W. Li, S. Mu, J. Du, Y. Yang, P. Tang, *Investigation of composition and structure for a novel Ti-Zr chemical conversion coating on 6063 aluminium alloy*, Progress in Organic Coatings, 2015, Volume 87, pp. 61-68.

[59] A. De Nicolo, L. Paussa, A. Gobessi, A. Lanzutti, C. Cepek, F. Andreatta, L. Fedrizzi, *Cerium conversion coating and sol-gel multilayer system for corrosion preotection of AA6060*, Surface & Coating Technology, 2016, Volume 287, pp.33-43.

[60] Z. Zou, N. Li, D. Li, H. Liu, S. Mu, *A vanadium-based conversion coating as chromate replacement for electrogalvanized steel substrates*, Journal of Alloys and Compounds, 2011, Volume 509, pp.503-507.

[61] S.A. Kulinich, A.S. Akhtar, D.Susac, P.C. Wong, K.C. Wong, K.A.R. Mitchell, *On the growth of conversion chromate coatings on 2024-Al*, Applied Surface Science, 2007, Volume 253, pp. 3144-3153.

[62] J.T. Qi, T. Hashimoto, J.R. Walton, X. Zhou, P. Skeldon, G.E. Thompson, *Trivalent chromium conversion coating formation on aluminium*, Surface and Coating Technology, Volume 280, 2015, pp. 317-329.

[63] I. Danilidis, J. Hunter, G.M. Scamans, J.M. Sykes, *Effect of inorganic additions on the performance of manganese-based conversion treatments*, Corrosion Science, Volume 49, 2007, pp. 1559-1569.

[64] J.W. Bibber: US Patent 5554231 (1996).

[65] S.A. Kulinich, A.S. Akhtar, P.C. Wong, K.C. Wong, K.A.R. Mitchell, *Growth of permanganate conversion coating on 2024-Al alloy*, Thin Solid Films, 2007, Volume 515, pp.8386-8392.

[66] X. Zhong, X. Wu, Y Jia, Y. Lui, *Self-repairing vanadium-zirconium composite conversion coating for aluminium alloys*, Applied Surface Science, Volume 280, 2013, pp. 489-493.

[67] W. Guixiang, Z. Milin, W. Ruizhi, *Molybdate and molybdate/permanganate conversion coatings on Mg-8.5Li alloy*, Applied Surface Science, Volume 258, 2012, pp. 2648-2654.

[68] M. Kendig, R. Buchheit, *Surface Conversions of Aluminum and Ferrous Alloys for Corrosion Resistance*, Process Corrosion, Research Topical Symposium CORROSION, NACE International, 2000, p1.

[69] L.S. Sander, E.M. Musingo, W.J. Neill, "*Nonchromate Bath for the Primer and Anticorrosion Coating on Aluminum Alloys*", U.S. Patent No. 5,401,333, 28 March 1995.

[70] S.E. Dolan, "*Chromium-Free Conversion Coating Composition and Process for Treating Metals*", U.S. Patent No. 5,449,415, 12 September 1995.

[71] A.H. Yi, W.F. Li, J. Du, S.L. Mu, *Preparation and properties of chrome-free colored Ti/Zr based conversion coating on aluminum alloy*, Applied Surface Science, 2012, Volume 258, pp. 5960-5964.

[72] A.J. MacAlister, J.L. Murry, *The (Al-Mn) Aluminum-Manganese System,* Bulletin of Alloy Phase Diagrams, 1987, Vol. 8 (5), pp.438-439.

11 Appendix 1: Higher magnification photos of Cr^{III}-Zr and Mn-V coated samples

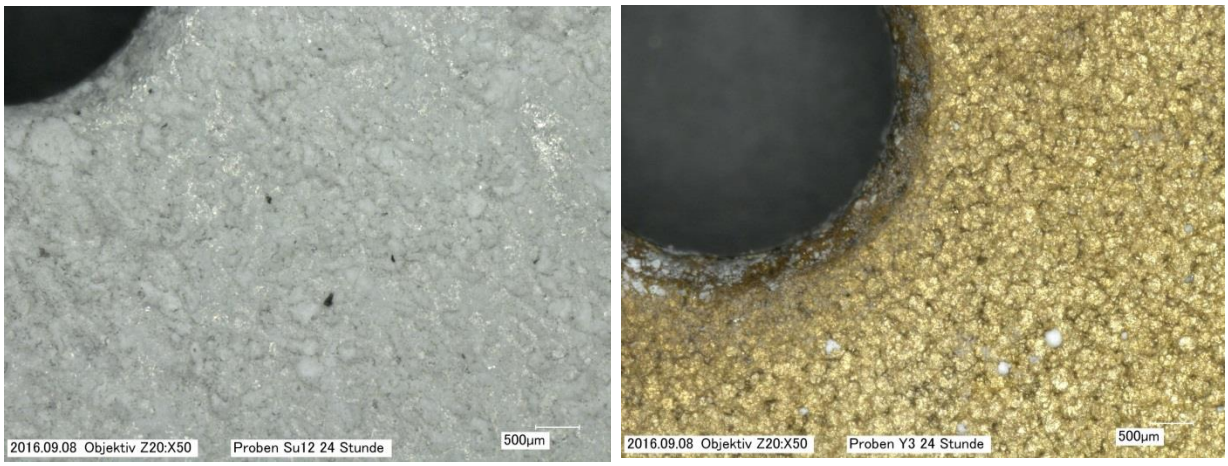

Figure 6.8-1: SurTec650 chromitAL (left) and PVCC coated (right) plates after 24 hours in the salt bath. (~50x magnification)

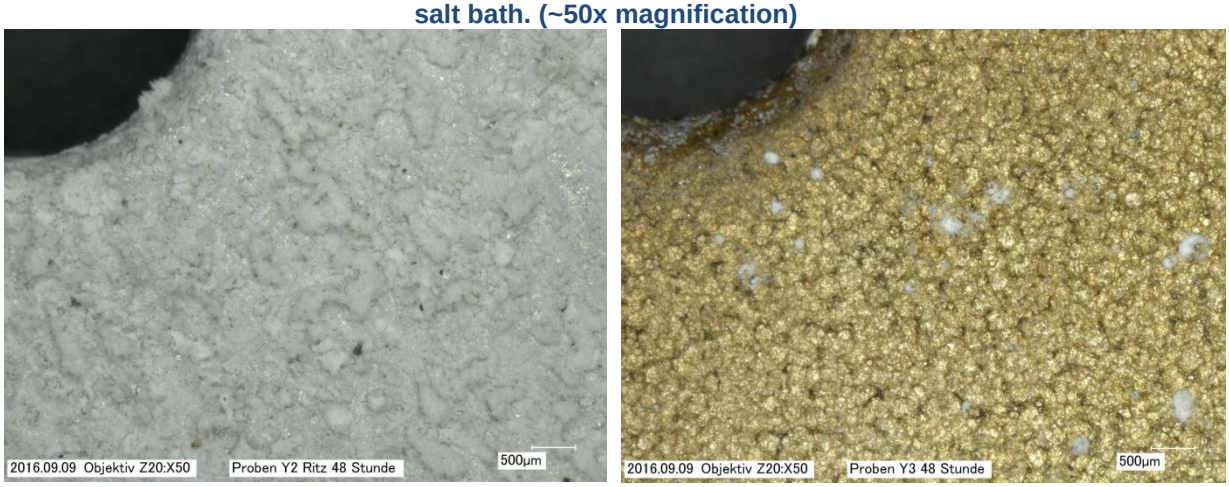

Figure 6.8-2: SurTec650 chromitAL (left) and PVCC coated (right) plates after 48 hours in the salt bath. (~50x magnification)

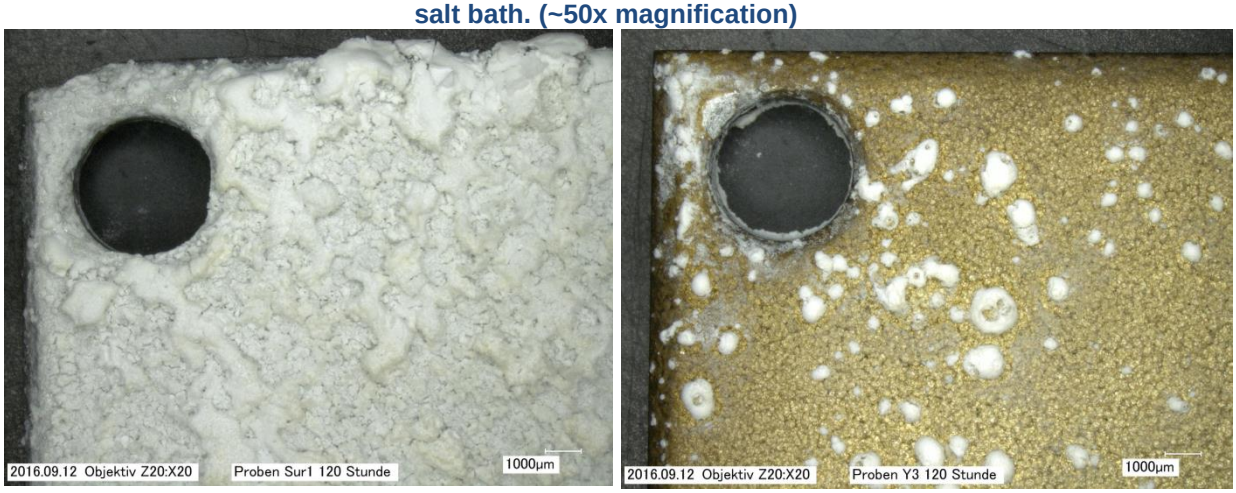

Figure 6.8-3: SurTec650 chromitAL (left) and PVCC coated (right) plates after 120 hours in the salt bath. (~20x magnification)

12 Appendix 2: Weight loss measurements of corrosion samples

Data of mass loss during corrosion tests			
Surface treatment	**Surface condition**	**Starting weight (g)**	**Final weight (g)**
PVCC	Plain	19.7112	19.6476
PVCC	Scribed	19.8505	19.7846
SurTec650	Plain	20.3700	20.2834
SurTec650	Scribed	20.7070	20.5950
Al + PVCC	Plain	18.9801	18.9659
Al + PVCC	Scribed	19.9650	19.9568
AlMn12 + PVCC	Plain	20.2548	20.2368
AlMn12 + PVCC	Scribed	19.9030	19.8933
Cadmium	Plain	8.6757	8.6604
Cadmium	Scribed	8.7112	8.6950
Cadmium + Cr^{VI}	Plain	8.5823	8.5717
Cadmium + Cr^{VI}	Scribed	8.3755	8.3622

13 Appendix 3: Hardness measurements of Al-Mn screening samples

Sample	**Measurement**						**Average**	**St. Dev.**
	1	**2**	**3**	**4**	**5**	**6**	**H_v(0.1)**	**H_v(0.1)**
Al	32	29	29.1	29.1	28.5	28.6	**29**	**1,3**
AlMn8	62.9	53.1	45.7	43.3	48.6	50.6	**51**	**6,9**
AlMn10	58.6	65.0	56.1	54.5	92.8	89.8	**69**	**17,3**
AlMn12	106	106	115	105	69.7	68.5	**95**	**20,4**
AlMn14	54.2	48.3	107	111	80.7	97.4	**83**	**26,9**
AlMn16	157	134	104	174	189	205	**144**	**37,1**
AlMn18	46.5	88.4	63.9	103	197	203	**117**	**67,2**
AlMn20	130	127	282	222	315	355	**239**	**95,7**
AlMn22	381	283	358	203	564	643	**405**	**167,6**

14 Appendix 4: Hardness measurements of AlMn12 APS samples

AlMn12 Sample	Measurement						Average
	1	2	3	4	5	6	$H_v(0.1)$
1	103	119	119	119	115	116	**115.2**
2	126	122					**124**
3	132	131	145	141	157	146	**142**
4	130	130					**130**
5	141	141	121	109	128	127	**127.8**
6	165	147					**156**
7	124	110	158	147	131	136	**134.3**
8	111	95.8					**103.4**
9	141	136					**138.5**
10	117	116					**116.5**
11	109	106					**107.5**
12	128	122					**125**
13	124	124					**124**
14	130	130					**130**
15	132	132					**132**
16	127	127					**127**
17	148	145					**146.5**
18	121	117					**119**